doi.org/10.26434/chemrxiv.12732011.v2

Highly Stable 1,2-Dicarbonyl Radical Cations Derived from N-Heterocyclic Carbenes

Youngsuk Kim, Jung Eun Byeon, Gu Yoon Jeong, Seoung Su Kim, Hayoung Song, Eunsung Lee

Submitted date: 10/05/2021 • Posted date: 11/05/2021

Citation information: Kim, Youngsuk; Byeon, Jung Eun; Jeong, Gu Yoon; Kim, Seoung Su; Song, Hayoung; Lee, Eunsung (2020): Highly Stable 1,2-Dicarbonyl Radical Cations Derived from N-Heterocyclic Carbenes. ChemRxiv. Preprint. https://doi.org/10.26434/chemrxiv.12732011.v2

The present manuscript describes the design, synthesis, and characterization of the most stable organic radical reported up to date.
Here we report: ▪ Synthesis and full characterization including X-ray structure of stable 1,2-dicarbonyl radicals ▪ Proposed mechanism for the formation of the presented radicals ▪ Redox reactivity of the radicals ▪ Stability of the radicals under various organic and inorganic conditions

File list (2)

Highly Stable 1,2-Dicarbonyl Radical Cations Derived from N-Heterocyclic Carbenes

Youngsuk Kim, Jung Eun Byeon, Gu Yoon Jeong, Seoung Su Kim, Hayoung Song, Eunsung Lee*

Department of Chemistry, Pohang University of Science and Technology (POSTECH), Pohang, 37673, Republic of Korea

ABSTRACT: Stable organic radicals have been of great academic interest not only in the context of fundamental understanding of reactive intermediates, but also because of numerous applications as functional materials. Apart from the early examples of triphenylmethyl and TEMPO derivatives, reports on air- and water-stable organic radicals are scarce, and their development remains a challenge. Herein, we present the design and synthesis of a novel organic radical based on a 1,2-dicarbonyl scaffold supported by *N*-heterocyclic carbenes (NHCs). The presented radical cations exhibit remarkable stability towards various harsh conditions, such as the presence of reactive chemicals (reductants, oxidants, strong acids, and bases) or high temperatures, by far exceeding the stability of triphenylmethyl and TEMPO radicals. In addition, physiological conditions including aqueous buffer and blood serum are tolerated. The steric and electronic stabilization provided by the two NHC moieties enabled the successful design of the highly stable radical.

Having an unpaired valence electron, organic radicals are often thermodynamically and kinetically unstable, making their isolation and structural characterization challenging. Since the 'radical' discovery of the triphenylmethyl radical – the first persistent organic radical – by Gomberg in 1900,[1–3] various strategies to stabilize organic radicals have been developed, leading to the successful preparation of other stable organic radicals including the most widely studied aminoxyl radicals (also known as nitroxyl radicals) (**Figure 1a**).[4–7] Air- and water-stable organic radicals are promising spin labels or contrast agents for bio-imaging applications. These applications include the development of gadolinium-free organic radical contrast agents for magnetic resonance imaging (MRI).[8–11] However, most currently known persistent radicals are not suitable for this purpose, due to decomposition in the presence of organic or biological reducing agents such as ascorbate (TEMPO radicals) or reaction with oxidants such as peroxides (triarylmethyl radicals).[12–15] One possible solution to this problem is to enhance the stability of aminoxyl derivatives by steric protection with supramolecular or polymeric chains.[16–17] On the other hand, the development of a new organic radical platform that is inherently stable towards various harsh conditions is an attractive alternative.

π-Conjugation enables the delocalization of spin density and hence increases radical stability.[18] Glyoxal derivatives, as one of the simplest π-conjugated molecules, have been reported to generate corresponding 1,2-dicarbonyl radical anions,[19] which are well-known redox-active ligands. Consequently, several metal complexes containing 1,2-dicarbonyl radical anions have been reported.[20,21] However, free 1,2-dicarbonyl radical anions are unstable, and have only been studied by spectroscopic and computational methods. For example, one-electron reduction of phenylglyoxal derivatives produced the corresponding 1,2-dicarbonyl radical anions which were detected by electron paramagnetic resonance (EPR).[19] Clearly, the increase in stability due to the π-conjugation alone is not sufficient to render these radicals persistent. Therefore, we postulated that further steric and electronic stabilization would be necessary to obtain a versatile organic radical based on the 1,2-dicarbonyl scaffold.

Stable singlet carbenes[22–28] are well known to facilitate the generation and utilization of unstable species,[29–31] such as main group[32] and organic radicals, including carbonyl,[33–40] propargyl,[41–43] and aminyl[44,45] derivatives. In this context, we designed 1,2-dicarbonyl radical cations supported by two *N*-heterocyclic carbenes (NHCs), which provide steric protection and delocalization of the spin density.

Herein, we report the synthesis and characterization of highly stable 1,2-dicarbonyl radical cations carrying two imidazolium substituents. The presented radical cations are stable under various harsh conditions including high temperature and the presence of a strong base. In addition, the radical cations showed superior stability compared to the widely used nitroxyl radicals toward common radical quenchers such as peroxide, thiol, and ascorbate.

The 1,2-dicarbonyl radical cations $\mathbf{2a}^{\bullet+}$ and $\mathbf{2b}^{\bullet+}$ can be easily synthesized from oxalyl chloride and the corresponding NHCs (**Figure 1b**). Under a N_2 atmosphere, the reaction of NHC **1a** (IMes; 1,3-bis-(2,4,6-trimethylphenyl)imidazol-2-ylidene) or **1b** (IDipp; 1,3-bis-(2,6-diisopropylphenyl)imidazol-2-ylidene) with substoichiometric amount of oxalyl chloride in THF produced $[\mathbf{2a}^{\bullet+}][Cl^-]$ or $[\mathbf{2b}^{\bullet+}][Cl^-]$, and a subsequent anion exchange afforded $[\mathbf{2a}^{\bullet+}][BF_4^-]$ or $[\mathbf{2b}^{\bullet+}][BF_4^-]$, respectively, as deep purple solids. The reaction involves the formation of the dication intermediate $[\mathbf{2a}^{2+}][Cl^-]_2$, followed by a spontaneous one-electron reduction. To scrutinize the source of the electron, dication $[\mathbf{2a}^{2+}][BF_4^-]_2$ was synthesized (see below) and reacted with potential electron sources. Indeed, when $[\mathbf{2a}^{2+}][BF_4^-]_2$ was reacted with soluble organic chloride sources, slow color change was observed and an EPR signal corresponds to $\mathbf{2a}^{\bullet+}$ was observed (Figures S1 and S2). This suggests that the chloride in the reaction mixture may act as a reductant in the formation of $\mathbf{2a}^{\bullet+}$.

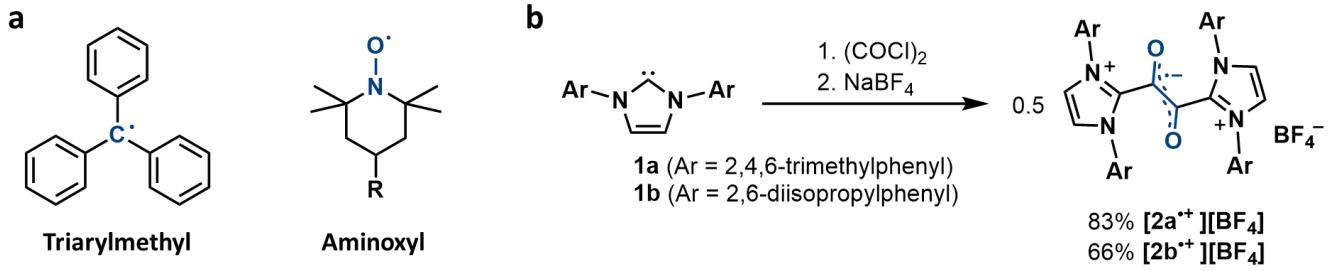

Figure 1. (a) State-of-the-art examples of the most widely used organic radicals. (b) This work: synthesis of the 1,2-dicarbonyl radical cations from NHCs and oxalyl chloride. Isolated yields were shown.

Single crystals suitable for X-ray crystallography were grown by slowly evaporating the mixed water/acetone solutions, enabling the determination of the molecular structures of [**2a**$^{\bullet+}$][BF_4^-] and [**2b**$^{\bullet+}$][BF_4^-] (**Figure 2a,b** and **Table S1**). The structural parameters for [**2a**$^{\bullet+}$][BF_4^-] and [**2b**$^{\bullet+}$][BF_4^-] are almost identical and well reproduced by DFT calculations on the M06/Def2-SV(P) level of theory (**Table S2**). The bond lengths of the central C_2O_2 unit indicate a bond order of 1.5 (O1–C2 1.245(2) Å; C2–C3 1.411(4) Å; C3–O2 1.245(2) Å for [**2a**$^{\bullet+}$][BF_4^-]). The planar structure of the central C_2O_2 unit also suggests π-delocalization of the radical electrons (torsion angle for O1–C2–C3–O2: 172.8(3)° for [**2a**$^{\bullet+}$][BF_4^-]). In addition, the calculated Wiberg bond orders were consistent with the single crystal X-ray structures (O1–C2 1.89; C2–C3 1.22; C3–O2 1.89 for [**2a**$^{\bullet+}$][BF_4^-], **Figure S7**).

In a typical case of singlet carbene-derived radicals,[46–58] a significant amount of spin density is delocalized over the carbene carbon and nitrogen atoms.[59] In contrast, DFT calculations suggest that **2a**$^{\bullet+}$ and **2b**$^{\bullet+}$ are very rare examples of NHC-derived radicals with minimal delocalization of the spin density over the NHC fragments. Very interestingly, 98% of the spin density of **2a**$^{\bullet+}$ is localized on the central C_2O_2 unit (O1 32%; C2 17%; C3 17%; O2 32%), with ca. ~1% of the spin density on the NHC nitrogen atoms. It is notable that Bertrand, Martin, and others studied a series of carbene-derived *α*-carbonyl radicals (or (amino)(carboxy)radicals), the stability of which could be well rationalized by the capto-dative effect[60] of their amino and carbonyl groups.[33–40] These radicals exhibit planar N–C–C–O motifs (with torsion angles less than 15°) and a significant delocalization (>50%) of spin densities over the carbene fragments.[35] Ghadwal and others reported carbene-derived radicals containing a redox-active C_2E_2 moiety (E = P or As) with extended π-conjugation,[61–67] having >20% of spin density on the carbene fragments. In stark contrast, our 1,2-dicarbonyl radicals have large N–C–C–O torsion angles (N–C1–C2–O1 for [**2a**$^{\bullet+}$][BF_4^-]: 53.0(3)°; [**2b**$^{\bullet+}$][BF_4^-]: 66.9(5)°) which results from the absence of conjugation of the π electrons between the dicarbonyl and the NHC fragments.

Experimental EPR spectra of [**2a**$^{\bullet+}$][BF_4^-] and [**2b**$^{\bullet+}$][BF_4^-] were nearly identical, and could be successfully simulated considering the splitting from the four nitrogen atoms characterized by small hyperfine coupling constants ($a(^{14}N)$ = 3.0, 3.0, 2.6, 2.6 MHz for [**2a**$^{\bullet+}$][BF_4^-]), in agreement with the small percentage of spin density on the nitrogen atoms (**Figure 2c**). The DFT calculated singly occupied molecular orbital (SOMO) of **2a**$^{\bullet+}$ (**Figure 2d**) well reproduced the typical Ψ_3 orbital of a conjugated system with four *p* orbitals (e.g., 1,3-butadiene). The UV-vis absorption spectrum of [**2a**$^{\bullet+}$][Cl^-] in distilled water at room temperature showed a peak at λ_{max} = 472 nm which was well approximated by time-dependent DFT calculations at the M06/Def2-SV(P) level of theory (calculated λ_{max} = 534 nm corresponding to a SOMO(α) to LUMO(α) transition, **Figure S15**). Interestingly, [**2a**$^{\bullet+}$][Cl^-] shows weak solvatochromism as its absorption was red-shifted in organic solvents (λ_{max} = 510 nm in acetonitrile; λ_{max} = 521 nm in dichloromethane, **Figure S17**).

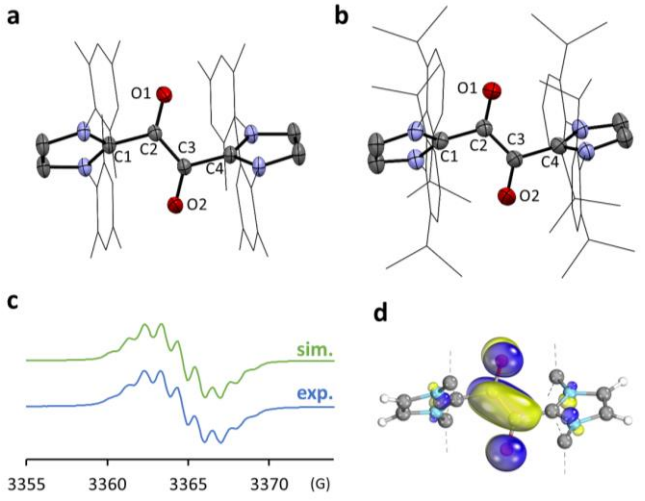

Figure 2. Characterization of the 1,2-dicarbonyl radical cations. (a) Solid-state structures of [**2a**$^{\bullet+}$][BF_4^-] and (b) [**2b**$^{\bullet+}$][BF_4^-] from single crystal X-ray crystallography. The thermal ellipsoids are shown at the 30% probability level. Anions, hydrogen atoms, solvent molecules and disorders were omitted for clarity. (c) Experimental (bottom) and simulated (top) EPR spectra of [**2a**$^{\bullet+}$][BF_4^-] (g = 2.0060; hyperfine coupling constants: $a(^{14}N)$ = 3.0, 3.0, 2.6, 2.6 MHz). (d) DFT calculated SOMO(*α*) of **2a**$^{\bullet+}$ (M06/Def2-SV(P); mesityl substituents were omitted for clarity.

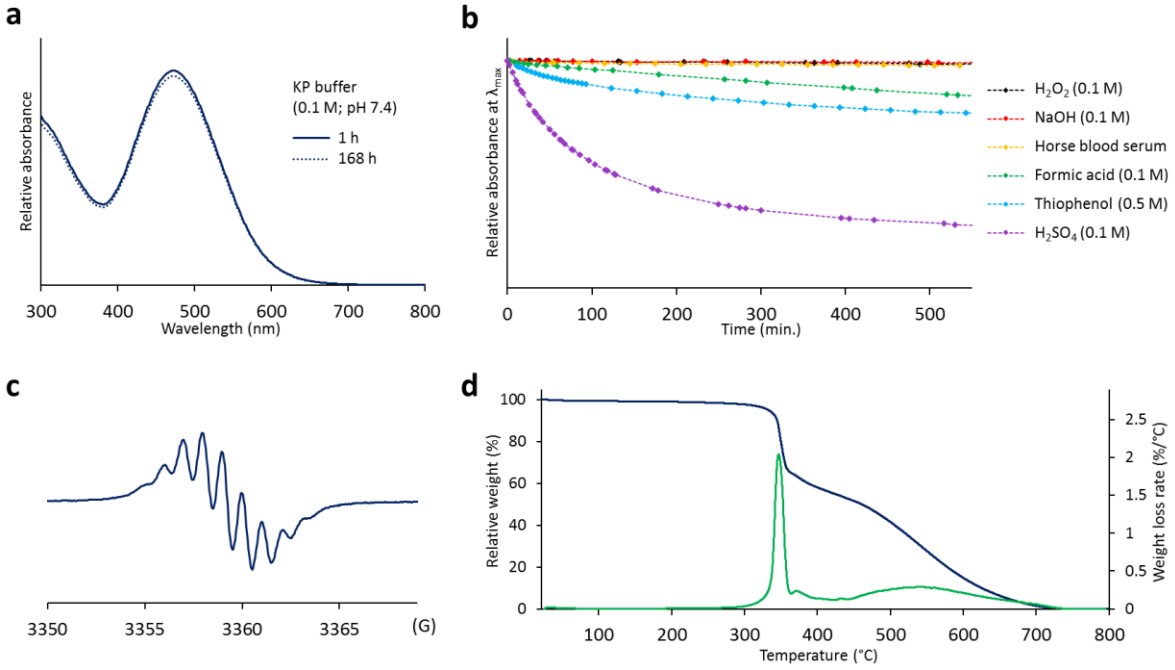

Figure 3. Stability of the 1,2-dicarbonyl radical cation. (a) UV-vis spectra of 0.16 mM [**2a**$^{\bullet+}$][Cl$^-$] in potassium phosphate buffer (0.1 M, pH 7.4) 1 h (solid line) and 168 h (dotted line) after dissolution. λ_{max} = 472 nm. (b) Decay of 0.16 mM [**2a**$^{\bullet+}$][Cl$^-$] in 0.1 M aqueous hydrogen peroxide (black, λ_{max} = 472 nm), 0.1 M aqueous sodium hydroxide (red, λ_{max} = 472 nm), horse blood serum (yellow, λ_{max} = 488 nm, serum(70%) mixed with distilled water(30%)), 0.1 M aqueous formic acid (green, λ_{max} = 472 nm), 0.5 M thiophenol in dichloromethane (blue, λ_{max} = 521 nm), and 0.1 M aqueous sulfuric acid (purple, λ_{max} = 472 nm). (c) EPR spectrum of [**2a**$^{\bullet+}$][Cl$^-$] after heating for 6 hours at 200 °C. (d) Thermal gravimetric analysis (dark blue) and differential thermal gravimetric (DTG) analysis (green) of [**2a**$^{\bullet+}$][Cl$^-$] under air.

To test the stability of the 1,2-dicarbonyl radical cations under physiological conditions, the concentration of [**2a**$^{\bullet+}$][Cl$^-$] in potassium phosphate buffer (0.1 M, pH 7.4) was monitored by UV-vis spectroscopy at λ_{max} = 472 nm. Surprisingly, [**2a**$^{\bullet+}$][Cl$^-$] showed high stability as less than 3% of the radical cation decomposed over 7 days, which corresponds to the half-life of ~4000 hours (**Figure 3a** and **Figure S18a**). In addition, even in the presence of excess sodium ascorbate (which is a common biological reducing agent known to be detrimental to organic radicals) in the buffer solution, [**2a**$^{\bullet+}$][Cl$^-$] showed high stability, showing a half-life of ~3000 hours (**Figure S18b**). Furthermore, [**2a**$^{\bullet+}$][Cl$^-$] remained stable under harsher conditions that most other organic radicals do not tolerate (**Figure 3b** and **Figure S19**). For instance, a solution of [**2a**$^{\bullet+}$][Cl$^-$] in horse blood serum showed only ca. 2% decrease of the UV-vis absorption signal over 500 minutes. [**2a**$^{\bullet+}$][Cl$^-$] also showed remarkable resistance towards highly basic or oxidizing conditions, as illustrated by the fact that in 0.1 M aqueous hydrogen peroxide or 0.1 M aqueous sodium hydroxide solutions, less than 2% of [**2a**$^{\bullet+}$][Cl$^-$] decomposed over 500 minutes. In the presence of high excess (0.5 M) of thiophenol in a dichloromethane solution, ~25% decomposition of [**2a**$^{\bullet+}$][Cl$^-$] was observed over 500 minutes, while in 0.1 M aqueous formic acid solution ~15% of [**2a**$^{\bullet+}$][Cl$^-$] decomposed during this time. Notably, [**2a**$^{\bullet+}$][Cl$^-$] showed half-life of ~2 hours even in a highly acidic 0.1 M aqueous sulfuric acid solution.

Furthermore, thermal stability of [**2a**$^{\bullet+}$][Cl$^-$] was studied by heating a solid sample up to 200 °C over 6 hours, and no sign of decomposition, such as a color change or a phase transition was observed. The EPR spectrum of [**2a**$^{\bullet+}$][Cl$^-$] after heating was identical to the spectrum of a freshly synthesized sample (**Figure 3c**). Thermal gravimetric analysis (TGA) of [**2a**$^{\bullet+}$][Cl$^-$] under air showed decomposition temperature of *ca*. 300 °C (**Figure 3d**), which is among the highest decomposition temperatures reported for organic radicals.[12]

The redox stability of the radical cations was further examined using cyclic voltammetry. The cyclic voltammograms of [**2a**$^{\bullet+}$][BF_4^-] and [**2b**$^{\bullet+}$][BF_4^-] showed reversible oxidation processes at $E_{1/2}$ = 0.51 and 0.49 V, respectively (vs. saturated Ag/AgCl electrode, **Figure S11**). Chemical oxidation of [**2a**$^{\bullet+}$][BF_4^-] was performed using $AgBF_4$ as an oxidant, providing the dication [**2a**$^{2+}$][BF_4^-]$_2$ (**Figure 4a**). Single crystal X-ray structure of [**2a**$^{2+}$][BF_4^-]$_2$ (**Figure 4b**) showed shortened O1–C2 (1.191(2) Å) and C3–O2 (1.201(2) Å), and elongated C2–C3 (1.536(5) Å) bonds, compared to [**2a**$^{\bullet+}$][BF_4^-]. In addition, the O1–C2–C3–O2 torsion angle was significantly reduced from 172.8(3)° in [**2a**$^{\bullet+}$][BF_4^-] to 156.9(4)° in [**2a**$^{2+}$][BF_4^-]$_2$, which also indicates the decrease in the strength of the C2–C3 π bonding interaction.

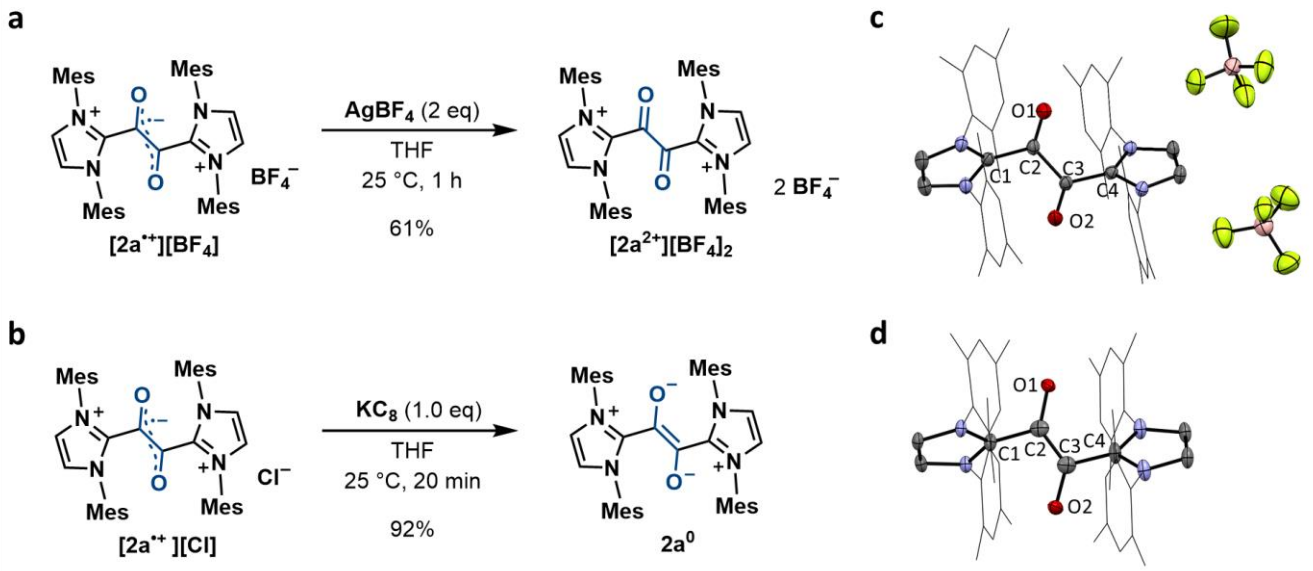

Figure 4. Redox behavior of the 1,2-dicarbonyl radical cations. (a) One electron oxidation of [**2a**$^{\bullet+}$][BF_4^-]. (b) One electron reduction of [**2a**$^{\bullet+}$][Cl^-]. (c) Solid-state structure of [**2a**$^{2+}$][BF_4^-]$_2$ and (d) **2a**^{0} from single crystal X-ray crystallography. The thermal ellipsoids are shown at the 30% probability level. Hydrogen atoms, solvent molecules, and disorders were omitted for clarity.

On the other hand, the radical cations were stable towards reduction potential down to –1 V (vs. Ag/AgCl) as indicated by cyclic voltammetry (**Figure S13**). The reduction process of **2a**$^{\bullet+}$ was found to be reversible ($E_{1/2}$ = –1.05 V; **Figure S12**), which corresponds to **2a**$^{\bullet+}$ + e^- ⇄ **2a**^{0}. Chemical reduction of [**2a**$^{\bullet+}$][Cl^-] using KC_8 as a reducing agent generated the corresponding neutral compound **2a**^{0} which was highly air- and moisture-sensitive (**Figure 4c**). Single crystal X-ray structure of **2a**^{0} (**Figure 4d**) showed longer O1–C2 (1.300(3) Å) and C3–O2 (1.311(3) Å), and shorter C2–C3 (1.349(4) Å) bonds, compared to **2a**$^{\bullet+}$. The solid-state structures of **2a**$^{2+}$ and **2a**^{0} were well reproduced with DFT calculations at M06/Def2-SV(P) level of theory (**Table S2**). The LUMO of **2a**$^{2+}$ and the HOMO of **2a**^{0} were nearly identical to the SOMO of **2a**$^{\bullet+}$, having a π-bonding interaction between C2–C3, and π-antibonding interactions between O1–C2 and C3–O2 (**Figure S6**).

Having highly stable and water-soluble organic radical cations in hand, we investigated a simple C–H deprotonation-deuteration reaction to demonstrate the stability of the radical cations during chemical reaction under harsh conditions. For instance, when [**2a**$^{\bullet+}$][Cl^-] was dissolved in D_2O with excess potassium carbonate or sodium hydroxide as a base and heated to 90 °C for 2 hours, complete deuteration of [**2a**$^{\bullet+}$][Cl^-] without decomposition was observed (See Supporting information for details).

In summary, highly stable and water-soluble 1,2-dicarbonyl radical cations **2a**$^{\bullet+}$ and **2b**$^{\bullet+}$ were synthesized and fully characterized. X-ray crystallography, EPR spectroscopy, and DFT calculations suggest that the unpaired electron is located on the central C_2O_2 unit, making these compounds rare and surprising examples of NHC-derived radicals with minimal delocalization of spin density over the NHC fragments. In addition, **2a**$^{\bullet+}$ and **2b**$^{\bullet+}$ showed remarkable stability towards various chemical and physiological conditions. For instance, the presented radical cations not only showed high resistance toward various radical quenchers including peroxide, thiol, and ascorbate, but also remained stable in presence of excess sodium hydroxide and under biological conditions (KP buffer and blood serum). A half-life of ca. 2 hours was measured even in 0.1 M sulfuric acid, and the thermal decomposition temperature was determined to be above 300 °C. These values are among the highest reported for organic radicals so far. Cyclic voltammetry showed that **2a**$^{\bullet+}$ and **2b**$^{\bullet+}$ are stable in the potential window between –1 V and +0.5 V (vs. saturated Ag/AgCl electrode). Stability of the presented radical cations is remarkable and counterintuitive as they do not enjoy π-delocalization over the NHC fragments, which is indeed common for NHC-derived stable radicals. This work demonstrates the successful design of stable radicals which was enabled by the redox-active dicarbonyl fragment and the NHC substituents providing suitable steric and electronic protection. We hope the new examples of highly stable organic radicals presented in this work would serve as a good platform for designing stable radicals and further promote the development of various functional materials for chemical and biological applications.

ASSOCIATED CONTENT

Supporting Information

The Supporting Information is available free of charge at https://pubs.acs.org/.

Supplementary figures and experimental details, including experimental procedures, syntheses, spectroscopic data, and theoretical calculations (PDF)

AUTHOR INFORMATION

Corresponding Author

*Email: eslee@postech.ac.kr

Author Contributions

The manuscript was written through contributions of all authors.

Notes

The authors declare the following competing financial interest: A patent application has been led through POSTECH on methods and reagents presented in this manuscript.

ACKNOWLEDGMENT

This work was supported by the National Supercomputing Center with supercomputing resources including technical support (KSC-2019-CRE-0162), and by the National Research Foundation of Korea (NRF-2019R1A2C2010732). X-ray diffraction experiment with synchrotron radiation was performed at the Pohang Accelerator Laboratory (Beamline 2D). High-resolution mass spectrometry was performed at the Korea Basic Science Institute (DS107). We thank Dr. Younghoon Kim for assistance with TGA, Dr. Dae Young Bae for assistance with IR, and Dr. Ewa Pietrasiak, Prof. Dr. Dmitry V. Yandulov, and Prof. Dr. David C. Powers for helpful discussions.

REFERENCES

(1) Gomberg, M. An Instance of Trivalent Carbon: Triphenylmethyl. *J. Am. Chem. Soc.* **1900,** *22*, 757-771.

(2) Griller, D.; Ingold, K. U. Persistent Carbon-Centered Radicals. *Acc. Chem. Res.* **1976,** *9*, 13-19.

(3) Leifert, D.; Studer, A. The Persistent Radical Effect in Organic Synthesis. *Angew. Chem. Int. Ed.* **2020,** *59*, 74-108.

(4) Forrester, A. R.; Thomson, R. H. Stable Nitroxide Radicals. *Nature* **1964,** *203*, 74-75.

(5) Back, O.; Celik, M. A.; Frenking, G.; Melaimi, M.; Donnadieu, B.; Bertrand, G. A Crystalline Phosphinyl Radical Cation. *J. Am. Chem. Soc.* **2010,** *132*, 10262-10263.

(6) Kato, K.; Osuka, A. Platforms for Stable Carbon-Centered Radicals. *Angew. Chem. Int. Ed.* **2019,** *58*, 8978-8986.

(7) Wilcox, D. A.; Agarkar, V.; Mukherjee, S.; Boudouris, B. W. Stable Radical Materials for Energy Applications. *Annu. Rev. Chem. Biomol. Eng.* **2018**, *9*, 83–103.

(8) Terreno, E.; Castelli, D. D.; Viale, A.; Aime, S. Challenges for Molecular Magnetic Resonance Imaging. *Chem. Rev.* **2010,** *110*, 3019-3042.

(9) Caravan, P.; Ellison, J. J.; McMurry, T. J.; Lauffer, R. B. Gadolinium(III) Chelates as MRI Contrast Agents: Structure, Dynamics, and Applications. *Chem. Rev.* **1999,** *99*, 2293-2352.

(10) Olchowy, C.; Cebulski, K.; Lasecki, M.; Chaber, R.; Olchowy, A.; Kalwak, K.; Zaleska-Dorobisz, U. The presence of the gadolinium-based contrast agent depositions in the brain and symptoms of gadolinium neurotoxicity - A systematic review. *PLoS One* **2017,** *12*, e0171704.

(11) Janzen, E. G.; Towner, R. A., Aminoxyl Radicals as MRI Contrast Agents. In *Bioactive Spin Labels*, Zhdanov, R. I., Ed. Springer Berlin Heidelberg: Berlin, Heidelberg, 1992; pp 573-583.

(12) Hicks, R. G. *Stable Radicals: Fundamentals and Applied Aspects of Odd-Electron Compounds*, Wiley, 2010; pp 521-535.

(13) Xia, S.; Villamena, F. A.; Hadad, C. M.; Kuppusamy, P.; Li, Y.; Zhu, H.; Zweier, J. L. Reactivity of Molecular Oxygen with Ethoxycarbonyl Derivatives of Tetrathiatriarylmethyl Radicals. *J. Org. Chem.* **2006,** *71*, 7268-7279.

(14) Frank, J.; Elewa, M.; Said, M. M.; El Shihawy, H. A.; El-Sadek, M.; Muller, D.; Meister, A.; Hause, G.; Drescher, S.; Metz, H.; Imming, P.; Mader, K. Synthesis, Characterization, and Nanoencapsulation of Tetrathiatriarylmethyl and Tetrachlorotriarylmethyl (Trityl) Radical Derivatives-A Study To Advance Their Applicability as in Vivo EPR Oxygen Sensors. *J. Org. Chem.* **2015,** *80*, 6754-6766.

(15) Hintz, H.; Vanas, A.; Klose, D.; Jeschke, G.; Godt, A. Trityl Radicals with a Combination of the Orthogonal Functional Groups Ethyne and Carboxyl: Synthesis without a Statistical Step and EPR Characterization. *J. Org. Chem.* **2019,** *84*, 3304-3320.

(16) Sowers, M. A.; McCombs, J. R.; Wang, Y.; Paletta, J. T.; Morton, S. W.; Dreaden, E. C.; Boska, M. D.; Ottaviani, M. F.; Hammond, P. T.; Rajca, A.; Johnson, J. A. Redox-responsive branched-bottlebrush polymers for in vivo MRI and fluorescence imaging. *Nat Commun* **2014,** *5*, 5460.

(17) Nguyen, H. V. T.; Detappe, A.; Harvey, P.; Gallagher, N.; Mathieu, C.; Agius, M. P.; Zavidij, O.; Wang, W.; Jiang, Y.; Rajca, A.; Jasanoff, A.; Ghobrial, I. M.; Ghoroghchian, P. P.; Johnson, J. A. Pro-organic radical contrast agents ("pro-ORCAs") for real-time MRI of pro-drug activation in biological systems. *Polymer Chemistry* **2020,** *11*, 4768-4779.

(18) Tang, B.; Zhao, J.; Xu, J.-F.; Zhang, X. Tuning the stability of organic radicals: from covalent approaches to non-covalent approaches. *Chem. Sci.* **2020,** *11*, 1192-1204.

(19) Russell, G. A.; Strom, E. T.; Talaty, E. R.; Weiner, S. A. Semidiones. I. Acyclic Semidione Radical Anions and Cations Containing a Single Aryl Substituent1. *J. Am. Chem. Soc.* **1966,** *88*, 1998-2004.

(20) Zanello, P.; Corsini, M. Homoleptic, mononuclear transition metal complexes of 1,2-dioxolenes: Updating their electrochemical-to-structural (X-ray) properties. *Coord. Chem. Rev.* **2006,** *250*, 2000-2022.

(21) Kirk, M. L.; Shultz, D. A. Transition metal complexes of donor–acceptor biradicals. *Coord. Chem. Rev.* **2013,** *257*, 218-233.

(22) Hopkinson, M. N.; Richter, C.; Schedler, M.; Glorius, F. An overview of N-heterocyclic carbenes. *Nature* **2014,** *510*, 485-496.

(23) Bourissou, D.; Guerret, O.; Gabbaï, F. P.; Bertrand, G. Stable Carbenes. *Chem. Rev.* **2000,** *100*, 39-92.

(24) Igau, A.; Grutzmacher, H.; Baceiredo, A.; Bertrand, G. Analogous α,α'-bis-carbenoid, Triply Bonded Species: Synthesis of a Stable λ3-Phosphino Carbene-λ5-phosphaacetylene. *J. Am. Chem. Soc.* **1988,** *110*, 6463-6466.

(25) Arduengo, A. J.; Harlow, R. L.; Kline, M. A Stable Crystalline Carbene. *J. Am. Chem. Soc.* **1991,** *113*, 361-363.

(26) Lavallo, V.; Canac, Y.; Prasang, C.; Donnadieu, B.; Bertrand, G. Stable Cyclic (Alkyl)(amino)carbenes as Rigid or Flexible, Bulky, Electron-rich Ligands for Transition-metal Catalysts: a Quaternary Carbon Atom Makes the Difference. *Angew. Chem. Int. Ed.* **2005,** *44*, 5705-5709.

(27) Melaimi, M.; Soleilhavoup, M.; Bertrand, G. Stable Cyclic Carbenes and Related Species beyond Diaminocarbenes. *Angew. Chem. Int. Ed.* **2010,** *49*, 8810-8849.

(28) Melaimi, M.; Jazzar, R.; Soleilhavoup, M.; Bertrand, G. Cyclic (Alkyl)(amino)carbenes (CAACs): Recent Developments. *Angew. Chem. Int. Ed.* **2017,** *56*, 10046-10068.

(29) Wang, Y.; Robinson, G. H. Carbene-stabilized main group diatomic allotropes. *Dalton Trans.* **2012,** *41*, 337-345.

(30) Chandra Mondal, K.; Roy, S.; Roesky, H. W. Silicon based radicals, radical ions, diradicals and diradicaloids. *Chem. Soc. Rev.* **2016,** *45*, 1080-1111.

(31) Yao, S.; Xiong, Y.; Driess, M. A New Area in Main-Group Chemistry: Zerovalent Monoatomic Silicon Compounds and Their Analogues. *Acc. Chem. Res.* **2017,** *50*, 2026-2037.

(32) Martin, C. D.; Soleilhavoup, M.; Bertrand, G. Carbene-Stabilized Main Group Radicals and Radical Ions. *Chem. Sci.* **2013,** *4*, 3020-3030.

(33) Mahoney, J. K.; Martin, D.; Moore, C. E.; Rheingold, A. L.; Bertrand, G. Bottleable (Amino)(Carboxy) Radicals Derived from Cyclic (Alkyl)(Amino) Carbenes. *J. Am. Chem. Soc.* **2013,** *135*, 18766-18769.

(34) Martin, D.; Moore, C. E.; Rheingold, A. L.; Bertrand, G. An Air-Stable Oxyallyl Radical Cation. *Angew. Chem. Int. Ed.* **2013,** *52*, 7014-7017.

(35) Mahoney, J. K.; Martin, D.; Thomas, F.; Moore, C. E.; Rheingold, A. L.; Bertrand, G. Air-Persistent Monomeric (Amino)(carboxy) Radicals Derived from Cyclic (Alkyl)(Amino) Carbenes. *J. Am. Chem. Soc.* **2015,** *137*, 7519-7525.

(36) Deardorff, C. L.; Eric Sikma, R.; Rhodes, C. P.; Hudnall, T. W. Carbene-derived alpha-acyl formamidinium cations: organic molecules with readily tunable multiple redox processes. *Chem. Commun.* **2016,** *52*, 9024-9027.

(37) Regnier, V.; Molton, F.; Philouze, C.; Martin, D. An air-persistent oxyallyl radical cation with simple di(methyl)amino substituents. *Chem. Commun.* **2016,** *52*, 11422-11425.

(38) Mahoney, J. K.; Jazzar, R.; Royal, G.; Martin, D.; Bertrand, G. The Advantages of Cyclic Over Acyclic Carbenes To Access Isolable Capto-Dative C-Centered Radicals. *Chem. Eur. J.* **2017,** *23*, 6206-6212.

(39) Regnier, V.; Romero, E. A.; Molton, F.; Jazzar, R.; Bertrand, G.; Martin, D. What Are the Radical Intermediates in Oxidative N-Heterocyclic Carbene Organocatalysis? *J. Am. Chem. Soc.* **2019,** *141*, 1109-1117.
(40) Mahoney, J. K.; Regnier, V.; Romero, E. A.; Molton, F.; Royal, G.; Jazzar, R.; Martin, D.; Bertrand, G. The serendipitous discovery of a readily available redox-bistable molecule derived from cyclic(alkyl)(amino)carbenes. *Org. Chem. Front.* **2018,** *5*, 2073-2078.
(41) Hansmann, M. M.; Melaimi, M.; Bertrand, G. Crystalline Monomeric Allenyl/Propargyl Radical. *J. Am. Chem. Soc.* **2017,** *139*, 15620-15623.
(42) Li, Y.; Mondal, K. C.; Samuel, P. P.; Zhu, H.; Orben, C. M.; Panneerselvam, S.; Dittrich, B.; Schwederski, B.; Kaim, W.; Mondal, T.; Koley, D.; Roesky, H. W. C_4 Cumulene and the Corresponding Air-Stable Radical Cation and Dication. *Angew. Chem. Int. Ed.* **2014,** *53*, 4168-4172.
(43) Hansmann, M. M.; Melaimi, M.; Bertrand, G. Organic Mixed Valence Compounds Derived from Cyclic (Alkyl)(amino)carbenes. *J. Am. Chem. Soc.* **2018,** *140*, 2206-2213.
(44) Eymann, L. Y. M.; Tskhovrebov, A. G.; Sienkiewicz, A.; Bila, J. L.; Zivkovic, I.; Ronnow, H. M.; Wodrich, M. D.; Vannay, L.; Corminboeuf, C.; Pattison, P.; Solari, E.; Scopelliti, R.; Severin, K. Neutral Aminyl Radicals Derived from Azoimidazolium Dyes. *J. Am. Chem. Soc.* **2016,** *138*, 15126-15129.
(45) Back, J.; Park, J.; Kim, Y.; Kang, H.; Kim, Y.; Park, M. J.; Kim, K.; Lee, E. Triazenyl Radicals Stabilized by N-Heterocyclic Carbenes. *J. Am. Chem. Soc.* **2017,** *139*, 15300-15303.
(46) Ueng, S. H.; Solovyev, A.; Yuan, X.; Geib, S. J.; Fensterbank, L.; Lacote, E.; Malacria, M.; Newcomb, M.; Walton, J. C.; Curran, D. P. *N*-Heterocyclic Carbene Boryl Radicals: A New Class of Boron-Centered Radical. *J. Am. Chem. Soc.* **2009,** *131*, 11256-11262.
(47) Matsumoto, T.; Gabbaï, F. P. A Borenium Cation Stabilized by an N-Heterocyclic Carbene Ligand. *Organometallics* **2009,** *28*, 4252-4253.
(48) Bissinger, P.; Braunschweig, H.; Damme, A.; Krummenacher, I.; Phukan, A. K.; Radacki, K.; Sugawara, S. Isolation of a Neutral Boron-Containing Radical Stabilized by a Cyclic (Alkyl)(Amino)Carbene. *Angew. Chem. Int. Ed.* **2014,** *53*, 7360-7363.
(49) Park, J.; Song, H.; Kim, Y.; Eun, B.; Kim, Y.; Bae, D. Y.; Park, S.; Rhee, Y. M.; Kim, W. J.; Kim, K.; Lee, E. *N*-Heterocyclic Carbene Nitric Oxide Radicals *J. Am. Chem. Soc.* **2015,** *137*, 4642-4645.
(50) Park, J. S.; Karnas, E.; Ohkubo, K.; Chen, P.; Kadish, K. M.; Fukuzumi, S.; Bielawski, C. W.; Hudnall, T. W.; Lynch, V. M.; Sessler, J. L. Ion-mediated electron transfer in a supramolecular donor-acceptor ensemble. *Science* **2010,** *329*, 1324-1327.
(51) Silva Valverde, M. F.; Schweyen, P.; Gisinger, D.; Bannenberg, T.; Freytag, M.; Kleeberg, C.; Tamm, M. N-Heterocyclic Carbene Stabilized Boryl Radicals. *Angew. Chem. Int. Ed.* **2017,** *56*, 1135-1140.
(52) Kim, Y.; Kim, K.; Lee, E. Oxime Ether Radical Cations Stabilized by N-Heterocyclic Carbenes. *Angew. Chem. Int. Ed.* **2018,** *57*, 262-265.
(53) Kim, Y.; Lee, E. An air-stable N-heterocyclic carbene iminoxyl borate radical zwitterion. *Chem. Commun.* **2018,** *54*, 6824-6827.
(54) Styra, S.; Melaimi, M.; Moore, C. E.; Rheingold, A. L.; Augenstein, T.; Breher, F.; Bertrand, G. Crystalline Cyclic (Alkyl)(amino)carbene-tetrafluoropyridyl Radical. *Chem. Eur. J.* **2015,** *21*, 8441-8446.
(55) Rottschafer, D.; Neumann, B.; Stammler, H. G.; van Gastel, M.; Andrada, D. M.; Ghadwal, R. S. Crystalline Radicals Derived from Classical N-Heterocyclic Carbenes. *Angew. Chem. Int. Ed.* **2018,** *57*, 4765-4768.
(56) Su, Y.; Kinjo, R. Boron-Containing Radical Species. *Coord. Chem. Rev.* **2017**, *352*, 346–378.
(57) Yang, Wenlong; Krantz, Kelsie E.; Freeman, Lucas A.; Dickie, Diane A.; Molino, Andrew; Frenking, Gernot; Pan, Sudip; Wilson, David J. D.; Gilliard, Robert J. Persistent Borafluorene Radicals. *Angew. Chem. Int. Ed.* **2020**, *59*, 3850-3852.
(58) Saalfrank, C.; Fantuzzi, F.; Kupfer, T.; Ritschel, B.; Hammond, K.; Krummenacher, I.; Bertermann, R.; Wirthensohn, R.; Finze, M.; Schmid, P.; Engel, V.; Engels, B.; Braunschweig, H. CAAC-Stabilized 9,10-Diboraanthracenes—Acenes With Open-Shell Singlet Biradical Ground States. *Angew. Chem. Int. Ed.* **2020**, *59*, 19338–19343.
(59) Kim, Y.; Lee, E. Stable Organic Radicals Derived from *N*-Heterocyclic Carbenes. *Chem. Eur. J.* **2018,** *24*, 19110-19121.
(60) Viehe, H. G.; Janousek, Z.; Merenyi, R.; Stella, L. The Captodative Effect. *Acc. Chem. Res.* **1985,** *18*, 148-154.
(61) Sharma, M. K.; Blomeyer, S.; Neumann, B.; Stammler, H. G.; van Gastel, M.; Hinz, A.; Ghadwal, R. S. Crystalline Divinyldiarsene Radical Cations and Dications. *Angew. Chem. Int. Ed.* **2019,** *58*, 17599-17603.
(62) Sharma, M. K.; Rottschafer, D.; Blomeyer, S.; Neumann, B.; Stammler, H. G.; van Gastel, M.; Hinz, A.; Ghadwal, R. S. Diphosphene radical cations and dications with a pi-conjugated C2P2C2-framework. *Chem. Commun.* **2019,** *55*, 10408-10411.
(63) Sharma, M. K.; Blomeyer, S.; Glodde, T.; Neumann, B.; Stammler, H.-G.; Hinz, A.; van Gastel, M.; Ghadwal, R. S. Isolation of singlet carbene derived 2-phospha-1,3-butadienes and their sequential one-electron oxidation to radical cations and dications. *Chem. Sci.* **2020,** *11*, 1975-1984.
(64) Sharma, M. K.; Blomeyer, S.; Neumann, B.; Stammler, H. G.; Hinz, A.; van Gastel, M.; Ghadwal, R. S. Isolation of singlet carbene derived 2-arsa-1,3-butadiene radical cations and dications. *Chem. Commun.* **2020,** *56*, 3575-3578.
(65) Abraham, M. Y.; Wang, Y.; Xie, Y.; Gilliard, R. J., Jr.; Wei, P.; Vaccaro, B. J.; Johnson, M. K.; Schaefer, H. F., 3rd; Schleyer, P. V.; Robinson, G. H. Oxidation of Carbene-Stabilized Diarsenic: Diarsene Dications and Diarsenic Radical Cations. *J. Am. Chem. Soc.* **2013,** *135*, 2486-2488.
(66) Back, O.; Donnadieu, B.; Parameswaran, P.; Frenking, G.; Bertrand, G. Isolation of crystalline carbene-stabilized P(2)-radical cations and P(2)-dications. *Nat. Chem.* **2010,** *2*, 369-373.
(67) Kinjo, R.; Donnadieu, B.; Bertrand, G. Isolation of a Carbene-Stabilized Phosphorus Mononitride and Its Radical Cation ($PN^{+\bullet}$). *Angew. Chem. Int. Ed.* **2010,** *49*, 5930-5933.

Electronic Supplementary Information

Highly Stable 1,2-Dicarbonyl Radical Cations Derived from N-Heterocyclic Carbenes

Youngsuk Kim,[a] Jung Eun Byeon,[a] Gu Yoon Jeong,[a] Seoungsu Kim,[a] Hayoung Song,[a] Eunsung Lee*[,a]

[a] Department of Chemistry, Pohang University of Science and Technology (POSTECH), Pohang, 37673, Republic of Korea

*E-mail: eslee@postech.ac.kr

Table of contents

Materials and Methods

1. General methods

All air- and moisture-insensitive reactions were carried out under an ambient atmosphere, magnetically stirred. All air- and moisture-sensitive manipulations were performed using oven-dried glassware, including standard Schlenk and glovebox techniques under an atmosphere of nitrogen. High resolution mass spectrometry was performed at the Korea Basic Science Institute with a JEOL JMS 700 high resolution mass spectrometer. Thermal gravimetric analyses (TGA) were performed under air with a Perkin Elmer Pyris 1. Elemental analyses were performed at Ulsan National Institute of Science and Technology (UNIST) Central Research Facilities with a Leco Truspec Micro elemental analyzer. ESI-MS spectrometry was performed with a Thermofisher LTQ XL Mass Spectrometer.

2. Reagents

IMes (**1a**), IDipp (**1b**), and $IMesH^+Cl^-$ were synthesized according to a reference.[1] Oxalyl chloride $(COCl)_2$ and all other chemicals were purchased from commercial sources and used as received unless otherwise specified. Horse blood serum was purchased from Sigma-Aldrich Korea (product No. H1138) and used as received. 3Å molecular sieves were activated at 240 ˚C under dynamic vacuum for overnight prior to use. Benzene, toluene, pentane, diethyl ether, and THF (tetrahydrofuran) was distilled from deep purple sodium benzophenone ketyl and stored over activated 3Å molecular sieves. Acetonitrile-d_3 (CD_3CN) was dried using activated 3Å molecular sieves.

Experimental Details

Synthesis of [2a•+][BF4–]

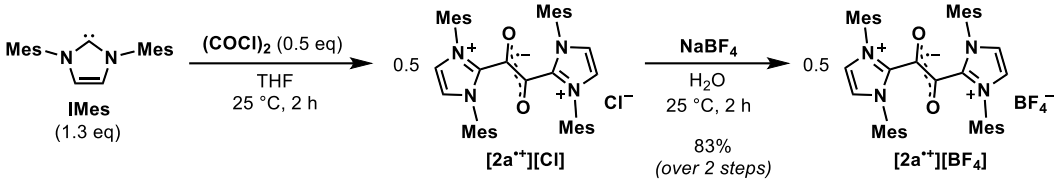

In a N_2 atmosphere glovebox, IMes (200 mg, 0.66 mmol, 1.3 eq) was placed in a 20 mL vial and subsequently dry THF (4 mL) was added to the vial. The solution was stirred at 25 °C, and dry THF solution (1 mL) of oxalyl chloride ($(COCl)_2$, 21.6 μL, 0.25 mmol, 0.5 eq) was slowly added. After 2 hours, the resulting precipitate was collected on a frit, washed with dry THF (3 × 3 mL) and dry diethyl ether (3 × 3 mL), and dried *in vacuo* to afford **[2a•+][Cl–]** as a purple solid. The obtained **[2a•+][Cl–]** was then suspended in distilled water (5 mL) and aqueous solution (1 mL) of sodium tetrafluoroborate ($NaBF_4$, 40 mg) was added. After 2 hours, the purple precipitate was collected on a frit, washed with distilled water (3 × 3 mL), and dried *in vacuo* to afford 158 mg of the product (83% over 2 steps). Single crystals of **[2a•+][Cl–]** suitable for X-ray crystallography were obtained from slow evaporation of water/acetone mixture solution. Single crystals of **[2a•+][BF4–]** suitable for X-ray crystallography were obtained from slow diffusion of pentane into dichloromethane solution. The radicals were NMR silent and their ^1H and ^{13}C spectra showed no meaningful data, except for a very broad peak in the 1H NMR around 2.5 ppm which we assigned as Ar–C**H**$_3$ from mesityl substituents. Data for **[2a•+][Cl–]**: ^1H NMR (500 MHz, Acetonitrile-d_3) δ 2.48 (br s, Ar–C**H**$_3$) ppm. UV absorption λ_{max} = 472 nm (water), 510 nm (acetonitrile), 521 nm (dichloromethane). EPR (microwave frequency = 9.4313 GHz) g_{iso} = 2.0062; hyperfine coupling constants: $a(^{14}N)$ = 3.0, 3.0, 2.6, 2.6 MHz. Data for **[2a•+][BF4–]**: m.p. 305 °C (decomp). IR(ATR): 1373 (C–O), 1052 (B–F) cm^{-1}. $^{19}F\{^1H\}$ NMR (282 MHz, Acetonitrile-d_3) δ –151.9 ppm. Anal. Calcd for $C_{44}H_{48}BF_4N_4O_2$: C, 70.31; H, 6.44; N, 7.45. Found: C, 69.99; H, 7.01; N, 7.48. HRMS (FAB): m/z calcd for $[C_{44}H_{48}N_4O_2\ (M)^+]$ 664.3777, found 664.3779. EPR (microwave frequency = 9.4467 GHz) g_{iso} = 2.0060; hyperfine coupling constants: $a(^{14}N)$ = 3.0, 3.0, 2.6, 2.6 MHz.

Synthesis of [2b•+][BF4–]

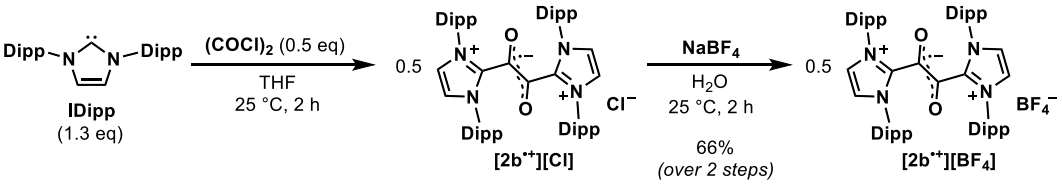

In a N_2 atmosphere glovebox, IDipp (100 mg, 0.26 mmol, 1.3 eq) was placed in a 20 mL vial and subsequently dry THF (2 mL) was added to the vial. The solution was stirred at 25 °C, and dry THF solution (1 mL) of oxalyl chloride ($(COCl)_2$, 8.4 μL, 0.10 mmol, 0.5 eq) was slowly added. After 2 hours, dry pentane (15 mL) was added, and the resulting precipitate was washed with diethyl ether (2 × 1 mL) and dried *in vacuo*. Further washing with distilled water (3 × 3 mL) afford **[2b•+][Cl–]** as a purple solid. The obtained **[2b•+][Cl–]** was then suspended in distilled water (1 mL) and aqueous

solution (1 mL) of sodium tetrafluoroborate ($NaBF_4$, 15 mg) was added. After 2 hours, the purple precipitate was collected on a frit, washed with distilled water (3 × 3 mL), and dried *in vacuo* to afford 60.4 mg of the product (66% over 2 steps). Single crystals of **[2b$^{\bullet+}$][BF_4^-]** suitable for X-ray crystallography were obtained from slow evaporation of water/acetone mixture solution. Data for **[2b$^{\bullet+}$][BF_4^-]**: m.p. 215 °C (decomp). $^{19}F\{^1H\}$ NMR (282 MHz, Acetonitrile-d_3) δ –151.9 ppm. Anal. Calcd for $C_{56}H_{72}BF_4N_4O_2$: C, 73.11; H, 7.89; N, 6.09 (*cf.* $C_{56}H_{72}BF_4N_4O_2 \cdot 2H_2O$: C, 70.35; H, 8.01; N, 5.86). Found: C, 70.39; H, 8.35; N, 5.67. HRMS (FAB): m/z calcd for [$C_{56}H_{72}N_4O_2$ $(M)^+$] 832.5655, found 832.5658. EPR (microwave frequency = 9.4413 GHz) g_{iso} = 2.0059; hyperfine coupling constants: $a(^{14}N)$ = 3.0, 3.0, 2.6, 2.6 MHz.

Synthesis of [2a^{2+}][BF_4^-]$_2$

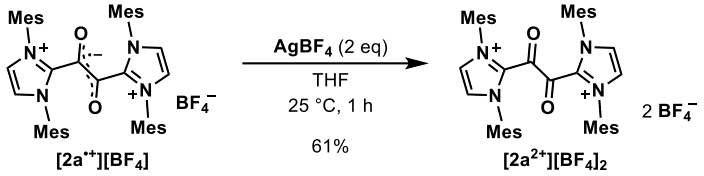

In a N_2 atmosphere glovebox, **[2a$^{\bullet+}$][BF_4^-]** (30 mg, 0.040 mmol) and silver(I) tetrafluoroborate ($AgBF_4$, 16 mg, 0.080 mmol, 2 eq) were placed in a 4 mL vial and subsequently dry THF (2 mL) was added to the vial. After 1 hour, the reaction mixture was centrifuged and decanted, and the remaining brown precipitate was dissolved in dry dichloromethane (3 mL). The solution was filtered through Celite to remove silver containing byproducts, and the filtrate was concentrated *in vacuo*. Dry pentane (3 mL) was added and the resulting precipitate was washed with dry THF (1 × 1 mL) and dry pentane (2 × 1 mL), and dried *in vacuo* to afford **[2a^{2+}][BF_4^-]$_2$** as an orange solid. (20 mg, 61%). ^1H NMR (500 MHz, Acetonitrile-d_3) δ 7.97 (s, 4H), 7.10 (s, 8H), 2.44 (s, 12H), 1.72 (s, 24H) ppm. $^{13}C\{^1H\}$ NMR (126 MHz, Acetonitrile-d_3) δ 172.4, 144.1, 135.6, 135.4, 131.3, 130.5, 129.6, 21.3, 17.2 ppm. $^{19}F\{^1H\}$ NMR (470 MHz, Acetonitrile-d_3) δ –151.8 ppm. Single crystals of **[2a^{2+}][BF_4^-]$_2$** suitable for X-ray crystallography were obtained from dichloromethane/pentane solution. m.p. 270 °C (decomp). IR(ATR): 1699 (C–O), 1056 (B–F) cm^{-1}. Anal. Calcd for $C_{44}H_{48}B_2F_8N_4O_2$: C, 63.03; H, 5.77 (*cf.* $C_{44}H_{48}B_2F_8N_4O_2 \cdot H_2O$: C, 61.70; H, 5.88; N, 6.54); N, 6.68. Found: C, 61.54; H, 6.24; N, 6.73.

Synthesis of 2a^0

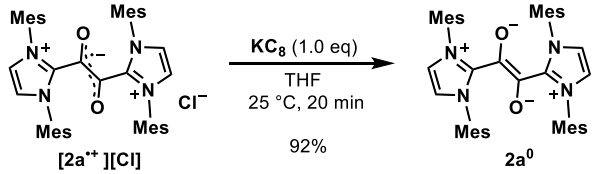

In a N_2 atmosphere glovebox, **[2a$^{\bullet+}$][Cl^-]** (10 mg, 0.014 mmol, 1.0 eq) and potassium graphite (KC_8, 1.9 mg, 0.014 mmol, 1.0 eq) were placed in a 4 mL vial and subsequently dry THF (0.8 mL) was added to the vial. The reaction mixture was quickly sonicated to dissolve the starting material. After 20 minutes at 25 °C, the reaction mixture was filtered to a thin pad of Celite and the resulting

filtrate was dried *in vacuo* to afford **2a⁰** as a dark green solid (8.7 mg; 92%). Single crystals of **2a⁰** suitable for X-ray crystallography were obtained from slow diffusion of pentane into the toluene solution. ^{1}H NMR (850 MHz, Benzene-d_6) δ 6.77 (s, 8H), 5.80 (s, 4H), 2.26 (s, 12H), 2.20 (s, 24H) ppm. ^{13}C{^{1}H} NMR (214 MHz, Benzene-d_6) δ 137.0, 126.6, 125.4, 124.8, 129.2, 128.8, 119.1, 21.3, 18.6 ppm. UV absorption λ_{max} = 394, 581 nm (benzene).

Mechanistic study

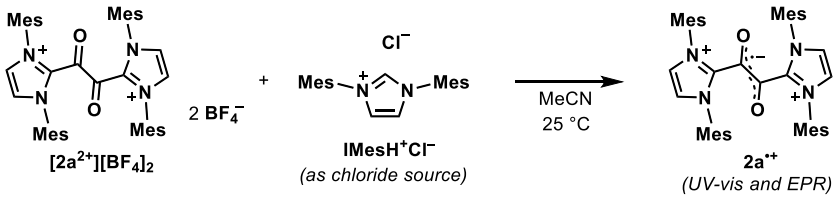

We proposed that the formation of **2a•⁺** from IMes and oxalyl chloride involves the formation of **2a²⁺** as an intermediate followed by a spontaneous one electron reduction. Interestingly, the reaction does not require additional reducing agent, therefore chloride or NHC in the reaction mixture may act as electron source. (Single electron transfer from NHCs to electron acceptors have been recently reported by Severin and co-workers.[2]) Indeed, the reaction between **[2a²⁺][BF₄⁻]₂** with IMesH⁺Cl⁻ (as a soluble chloride source) afforded **2a•⁺** which was detected by EPR and UV-vis spectroscopy.

In a N_2 atmosphere glovebox, **[2a²⁺][BF₄⁻]₂** (2.5 mg) and IMesH⁺Cl⁻ (5.0 mg, ca. 5 eq.) were dissolved in dry acetonitrile (3 mL). The reaction mixture was monitored by UV-vis which showed the slow formation of **2a•⁺** (**Figure S1**). EPR study also showed the existence of **2a•⁺** in the reaction mixture (**Figure S2**). The same reaction with tetrabutylammonium chloride as a chloride source instead of the imidazolium chloride gave identical results.

DFT calculation at M06/Def2-SV(P) level of theory with SMD model showed the electron transfer process from **2a²⁺** to chloride to generate **2a•⁺** and 0.5 Cl_2 is thermodynamically favorable (6.9 kcal/mol in THF and 5.2 kcal/mol in acetonitrile). (Balanced equation: **2a²⁺** • Cl^- → **2a•⁺** + 0.5 Cl_2)

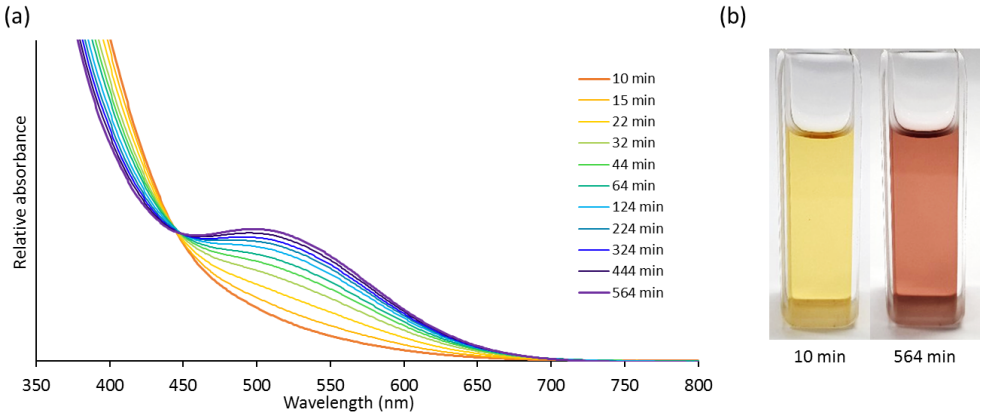

Figure S1. Monitoring of the formation of **2a•⁺** (corresponds to λ_{max} = 510 nm in acetonitrile) from the reaction between **[2a²⁺][BF₄⁻]₂** and IMesH⁺Cl⁻. (a) Selected spectra. (b) Color of the reaction mixture.

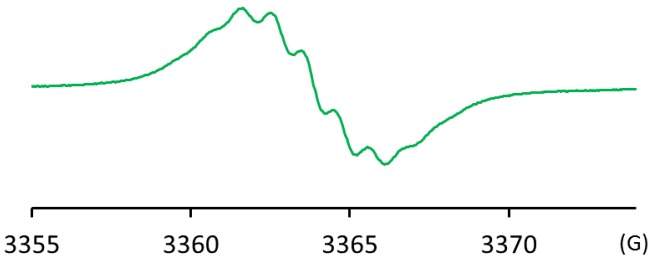

Figure S2. Experimental EPR spectra of the reaction mixture from the reaction between **[2a^{2+}][BF$_4^-$]$_2$** and IMesH$^+$Cl$^-$ at microwave frequency = 9.4452 GHz.

Deuteration

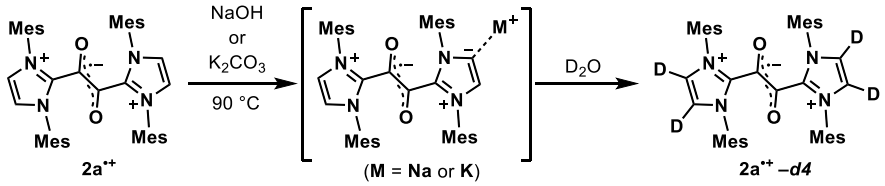

To demonstrate the radical can undergo post-synthetic modification even under harsh condition, the imidazolium C–H bonds of **2a**$^{\bullet+}$ were deuterated. Under ambient atmosphere, **[2a**$^{\bullet+}$**][Cl**$^-$**]** (0.4 mg) and excess NaOH (11 mg) or K_2CO_3 (14 mg) were dissolved in D_2O (1 mL). The reaction mixture was heated to 90 °C. No color change was observed during the reaction. After 2 hours, the reaction mixtures were diluted and analyzed by ESI-MS spectrometry (**Figure S3** and **Figure S4**) which showed complete deuteration toward **2a**$^{\bullet+}$-*d*$_4$.

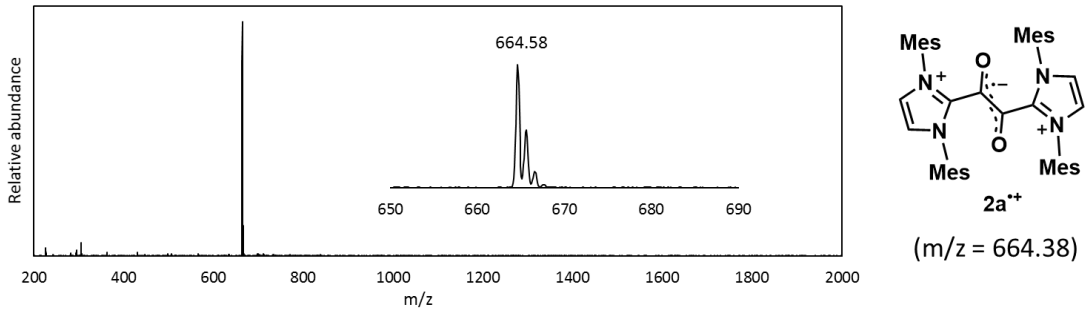

Figure S3. Experimental ESI-MS spectrum and expected mass of **2a**$^{\bullet+}$.

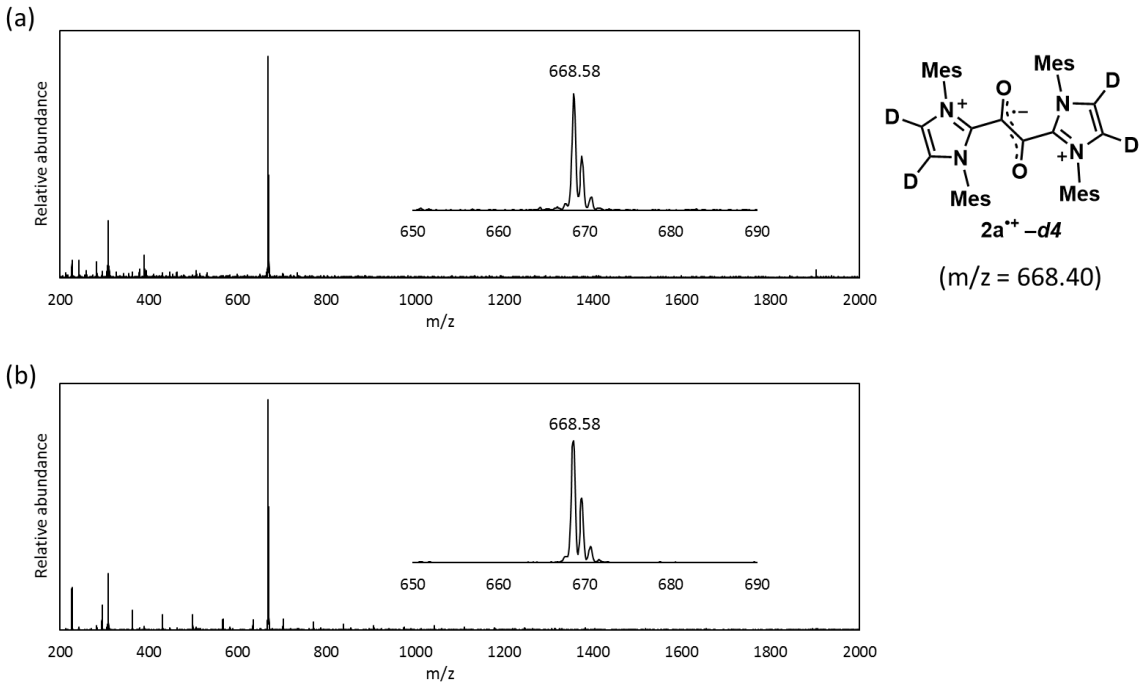

Figure S4. Experimental ESI-MS spectrum and expected mass of **2a**$^{\bullet+}$-d_4. (a) Deuteration with K_2CO_3. (b) Deuteration with NaOH.

DFT Calculation

General information

Geometry optimizations and frequency calculations were performed using Gaussian16[3] with M06 functional[4] and either Def2-SV(P)[5] or 6-31G(d,p)[6] basis set. In the geometry optimization, the default tight convergence in the SCF cycle was used without any orbital symmetry constraints. Solvation free energies were calculated using the SMD model.[7] Multiwfn[8] and IBOview[9] programs were used to visualize Molecular orbitals. Wiberg bond indices (WBIs) were calculated from the optimized geometry with Löwdin orthogonalization method using Multiwfn.

Coordinates of optimized structures

The following optimized geometries were displayed in Cartesian coordinates (atomic unit). E° represents the electronic energy of the optimized structure, and G° represents the sum of electronic and thermal free energies in Hartree unit.

2a$^{\bullet+}$ [E° = –2071.7768846; G° = –2071.044877; G°(THF) = –2071.1192563; G°(MeCN) = –2071.1267336] Def2-SV(P)

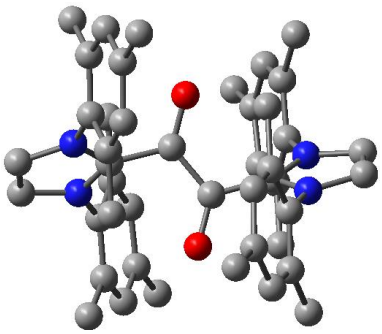

Charge = 1; Multiplicity = 2;

	Atomic coordinates (Cartesian; in atomic unit)			Mulliken charge	Spin density
O	-0.0171840011	0.8480612757	1.5432186703	-0.276975	0.322261
N	0.9531572985	2.2329742473	-1.4784521889	-0.177772	0.009341
N	-0.9732981757	2.7149840828	-0.6067925669	-0.181867	0.010149
C	2.4091076556	0.9420679413	-2.9519629225	0.086987	0.001577
C	2.2240605153	1.6070448015	-1.7292426389	-0.033928	-0.006434
C	0.0674792475	0.6436473770	0.3141463414	0.057964	0.179057
C	0.0239353394	1.8160944269	-0.6057497206	0.211481	-0.013777
C	3.6594787054	0.3698623447	-3.1785927654	-0.267071	0.003125
C	4.4690840987	1.1616235332	-1.0586920815	-0.242914	0.003365
C	3.2287593904	1.7339466230	-0.7630879147	0.085223	0.001990
C	4.7009967215	0.4707424115	-2.2484056471	0.107455	0.000364
C	0.5381273926	3.4256784095	-2.0427983886	0.012016	0.003733
C	-2.2305941130	2.5600911385	0.0775994805	-0.043861	-0.008295
C	-2.3963838824	3.1573589226	1.3315699438	0.105454	0.000265
C	-3.2298121400	1.8136799597	-0.5628971253	0.088162	0.003793
C	1.3143751224	0.8558351169	-3.9700781496	-0.278345	0.000132
C	-0.6723327553	3.7241587113	-1.5004434161	0.013144	0.000767
C	2.9946659818	2.4244000795	0.5467265236	-0.294230	-0.000158
C	6.0273876254	-0.1670551985	-2.5274792053	-0.291789	-0.000059
C	-4.6760882124	2.2816219918	1.3497569549	0.122873	-0.001051
C	-4.4536717854	1.7015103860	0.0963008306	-0.268962	0.002714
C	-2.9850936263	1.1408374659	-1.8800608933	-0.298792	0.001719

C	-3.6370766596	2.9965040076	1.9520802272	-0.264024	0.002089
C	-1.2722244549	3.8971478463	1.9866562079	-0.288616	0.000063
C	-6.0083484105	2.1367095349	2.0191393656	-0.293721	0.000045
O	0.0450386338	-0.8532861446	-1.5451881478	-0.274910	0.317473
N	0.9682139312	-2.2346430762	1.4780615542	-0.178061	0.008064
N	-0.9645257917	-2.7055824915	0.6155195095	-0.181705	0.008586
C	2.4261572893	-0.9418372919	2.9474275757	0.085212	0.001568
C	2.2414972536	-1.6128206725	1.7277742437	-0.035259	-0.005856
C	0.0887147157	-0.6426759186	-0.3160563645	0.060895	0.174180
C	0.0383976666	-1.8137499237	0.6085238373	0.212034	-0.013737
C	3.6783486717	-0.3737196800	3.1741596320	-0.266952	0.002665
C	4.4901718635	-1.1813863376	1.0609090934	-0.244279	0.002927
C	3.2482470968	-1.7502256497	0.7652188719	0.086841	0.001617
C	4.7217101734	-0.4842579349	2.2470516488	0.107347	0.000506
C	0.5477861985	-3.4233912138	2.0468923757	0.012035	0.003265
C	-2.2196681515	-2.5501033664	-0.0728717905	-0.045460	-0.007569
C	-2.3792667095	-3.1459445462	-1.3285783608	0.104887	0.000113
C	-3.2228628894	-1.8067274646	0.5650823993	0.088059	0.003239
C	1.3277353953	-0.8438509937	3.9607146171	-0.279997	0.000243
C	-0.6666785984	-3.7151261959	1.5100236738	0.013084	0.000432
C	3.0137801473	-2.4463548319	-0.5413489036	-0.294767	0.000190
C	6.0492842031	0.1516004232	2.5247718984	-0.291574	-0.000064
C	-4.6607342504	-2.2751666286	-1.3540590849	0.122729	-0.001094
C	-4.4443003572	-1.6962746954	-0.0989784656	-0.268678	0.002873
C	-2.9851946875	-1.1351507506	1.8840796445	-0.300387	0.001773
C	-3.6178478324	-2.9866973595	-1.9537064162	-0.263966	0.002218
C	-1.2512251705	-3.8833086432	-1.9800346042	-0.289807	0.000106
C	-5.9910309405	-2.1332838554	-2.0279831065	-0.293847	0.000045
H	3.8317012147	-0.1654768586	-4.1221151064	0.070696	-0.000165
H	5.2824065994	1.2628719938	-0.3276848581	0.055156	-0.000145
H	1.1582939485	3.9516630015	-2.7685913803	0.148413	-0.000102
H	0.3650257985	0.5334715365	-3.5048046940	0.155291	-0.001472
H	1.5713978993	0.1288258259	-4.7589619131	0.131561	0.000030
H	1.1388005612	1.8282621336	-4.4710468634	0.134084	0.000267
H	-1.3590170283	4.5547008771	-1.6656395769	0.148673	0.000160
H	2.3399054669	3.3121660621	0.4497993634	0.123237	0.000351
H	3.9492546739	2.7583575514	0.9899797818	0.137414	0.000098
H	2.5119923612	1.7453003246	1.2803583564	0.178205	-0.002899
H	5.9434354543	-1.2716775135	-2.5420020339	0.142645	0.000036
H	6.7818766630	0.1028438816	-1.7673387793	0.128512	-0.000002
H	6.4214581411	0.1313432420	-3.5166129787	0.149157	0.000022
H	-5.2648045298	1.1437080324	-0.3913640467	0.056835	-0.000148
H	-2.5821577851	1.8380279520	-2.6409819950	0.133316	0.000209
H	-3.9193244949	0.7101806190	-2.2807079016	0.132498	0.000126
H	-2.2546236949	0.3090113819	-1.7900628757	0.173171	-0.004960
H	-3.7948824908	3.4466638132	2.9408577139	0.070789	-0.000099
H	-0.4175994978	3.2124856766	2.1572794469	0.159792	-0.001657
H	-1.5829656261	4.3122489858	2.9600787092	0.131167	-0.000003
H	-0.9092277590	4.7390517369	1.3654504647	0.129980	-0.000009
H	-6.7652338221	2.7934029938	1.5483151435	0.153500	-0.000033
H	-5.9624728469	2.4027326059	3.0893594565	0.133675	-0.000004
H	-6.3907559489	1.1014627539	1.9378911605	0.133179	-0.000018
H	3.8503194711	0.1666981240	4.1148385297	0.070891	-0.000144
H	5.3047999237	-1.2892980079	0.3322310723	0.056081	-0.000118
H	1.1671362983	-3.9512315958	2.7720554134	0.148491	-0.000066
H	0.3824224081	-0.5163238818	3.4903323542	0.157241	-0.001677
H	1.5869475947	-0.1161534696	4.7482510592	0.131517	0.000024
H	1.1429291053	-1.8132832466	4.4641594120	0.134200	0.000299
H	-1.3579454475	-4.5410615212	1.6791221961	0.148758	0.000180
H	2.3544107279	-3.3303196345	-0.4411274991	0.123134	0.000304
H	3.9676266549	-2.7873201826	-0.9807433443	0.137352	0.000074
H	2.5351253701	-1.7687758814	-1.2790313149	0.178392	-0.002769
H	5.9672830290	1.2564271204	2.5355810917	0.142702	0.000040
H	6.8035153568	-0.1221056541	1.7657572082	0.128572	-0.000001
H	6.4423589001	-0.1443211695	3.5150535168	0.149333	0.000026
H	-5.2584021946	-1.1407521846	0.3863361519	0.056907	-0.000154

H	-2.5832789483	-1.8323578259	2.6455216867	0.132888	0.000181
H	-3.9224275095	-0.7079294588	2.2814253008	0.131950	0.000103
H	-2.2561490394	-0.3016188725	1.7982068532	0.175440	-0.004527
H	-3.7709799198	-3.4359122512	-2.9436478978	0.070847	-0.000109
H	-0.3967774988	-3.1974242456	-2.1474080548	0.161032	-0.001722
H	-1.5579122551	-4.2985835004	-2.9546713922	0.131215	-0.000004
H	-0.8893112421	-4.7249477061	-1.3577772067	0.130087	-0.000003
H	-6.7460036247	-2.7973811929	-1.5644968419	0.153709	-0.000034
H	-5.9393347552	-2.3923445976	-3.0996591041	0.133706	-0.000004
H	-6.3798044011	-1.1008649674	-1.9416280357	0.133241	-0.000018

2a$^{\bullet+}$ [E° = –2073.4773383; G° = –2072.741530] 6-31G(d,p)

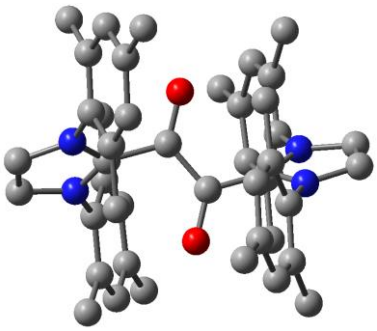

Charge = 1; Multiplicity = 2;

	Atomic coordinates (Cartesian; in atomic unit)			Isotropic Fermi Contact Couplings (Hyperfine coupling constants; MHz)
O	0.040199	0.865488	1.539833	-39.1021
N	0.96107	2.219707	-1.49551	3.03327
N	-0.96978	2.694625	-0.63654	2.80036
C	2.429092	0.928759	-2.95187	0.12768
C	2.239687	1.600492	-1.73708	-1.06926
C	0.083386	0.640677	0.307733	-6.72775
C	0.032062	1.802708	-0.624	-12.5269
C	3.684571	0.37504	-3.17761	0.24807
C	4.482676	1.187367	-1.06547	0.10855
C	3.237514	1.742408	-0.77134	-0.38423
C	4.723398	0.500193	-2.25158	-0.01659
C	0.539097	3.405743	-2.07186	-0.20797
C	-2.22349	2.545896	0.06017	-0.30265
C	-2.37119	3.154686	1.307593	0.0212
C	-3.22576	1.793501	-0.56027	-0.32943
C	1.327708	0.806745	-3.95927	-0.32037
C	-0.67227	3.698887	-1.53876	-0.36754
C	2.995511	2.426995	0.53979	-0.29068
C	6.066744	-0.09864	-2.53726	-0.0225
C	-4.64795	2.291911	1.355623	-0.10355
C	-4.44058	1.693861	0.111783	0.23045
C	-2.99657	1.0966	-1.8676	0.40566
C	-3.6035	3.00742	1.940298	0.21428
C	-1.23486	3.889045	1.947738	-0.38965
C	-5.97477	2.165789	2.039837	0.01886
O	-0.02901	-0.86583	-1.54115	-39.6671
N	0.943923	-2.22109	1.493849	3.06855
N	-0.98048	-2.70828	0.625841	2.81906
C	2.406547	-0.93065	2.956443	0.05948
C	2.21881	-1.59542	1.737685	-1.12132
C	0.059849	-0.64664	-0.30947	-6.12269
C	0.015712	-1.8093	0.618411	-12.7255
C	3.658768	-0.3701	3.183205	0.30851
C	4.457391	-1.16135	1.063536	0.15268
C	3.21542	-1.72322	0.768676	-0.41422
C	4.696393	-0.48152	2.254162	-0.03615

C	0.527256	-3.41054	2.066906	-0.20771
C	-2.23707	-2.55894	-0.06542	-0.34175
C	-2.39346	-3.16979	-1.31051	0.05087
C	-3.23288	-1.8002	0.557471	-0.27335
C	1.308518	-0.82459	3.969005	-0.35005
C	-0.68012	-3.71097	1.528627	-0.38311
C	2.976891	-2.40289	-0.54586	-0.43237
C	6.037244	0.121443	2.542952	-0.01957
C	-4.66619	-2.2959	-1.35056	-0.10034
C	-4.45032	-1.69598	-0.10912	0.22887
C	-2.99397	-1.1017	1.862334	0.40721
C	-3.62796	-3.01833	-1.93783	0.21007
C	-1.26308	-3.90952	-1.95464	-0.40172
C	-5.99501	-2.16418	-2.02978	0.0184
H	3.861292	-0.16347	-4.10876	-0.16393
H	5.287225	1.297241	-0.33796	-0.09448
H	1.152696	3.9249	-2.79351	0.05909
H	0.399388	0.473963	-3.48075	0.62076
H	1.593544	0.080535	-4.73212	0.05441
H	1.128899	1.760409	-4.4649	0.41554
H	-1.3581	4.515526	-1.71201	0.45181
H	2.325821	3.291296	0.446833	0.08303
H	3.93826	2.778351	0.969791	0.1442
H	2.536728	1.739776	1.266414	1.03193
H	5.985591	-1.17161	-2.74985	0.08202
H	6.754468	0.029197	-1.69469	-0.00402
H	6.529565	0.363411	-3.417	0.10322
H	-5.2512	1.132246	-0.35366	-0.13496
H	-2.58444	1.769409	-2.63065	0.0075
H	-3.93324	0.683325	-2.25378	0.23069
H	-2.28814	0.260386	-1.76461	0.95065
H	-3.74952	3.46485	2.918302	-0.13807
H	-0.40014	3.197263	2.12691	0.31872
H	-1.53836	4.322299	2.904287	0.0125
H	-0.86246	4.704465	1.314878	0.0345
H	-6.70684	2.8608	1.610873	-0.08795
H	-5.90193	2.385563	3.109134	-0.01166
H	-6.38871	1.156794	1.926018	-0.04076
H	3.834166	0.162273	4.118118	-0.20221
H	5.260915	-1.26062	0.333379	-0.13193
H	1.141523	-3.92722	2.789741	-0.02501
H	0.376301	-0.49551	3.496193	0.56775
H	1.57159	-0.10146	4.745667	0.06154
H	1.118993	-1.78311	4.468931	0.3358
H	-1.36143	-4.53201	1.698952	0.39947
H	2.311915	-3.27121	-0.45705	0.13646
H	3.921587	-2.74734	-0.97731	0.20433
H	2.515591	-1.71499	-1.27017	1.15442
H	5.951868	1.192428	2.763622	0.07173
H	6.725073	0.002376	1.699173	-0.00505
H	6.502641	-0.3451	3.41897	0.09285
H	-5.256	-1.12916	0.358574	-0.11866
H	-2.58551	-1.77614	2.625942	0.0387
H	-3.92584	-0.67953	2.250436	0.2866
H	-2.27948	-0.27109	1.75531	1.13823
H	-3.78045	-3.47699	-2.91428	-0.12524
H	-0.42581	-3.22147	-2.13554	0.30622
H	-1.57145	-4.34006	-2.91086	0.01721
H	-0.89287	-4.72754	-1.32393	0.02485
H	-6.72762	-2.8584	-1.60042	-0.08622
H	-5.92637	-2.38118	-3.09993	-0.01136
H	-6.40561	-1.1543	-1.91181	-0.04056

2a^{2+} [E° = –2071.4621977; G° = –2070.733418] Def2-SV(P)

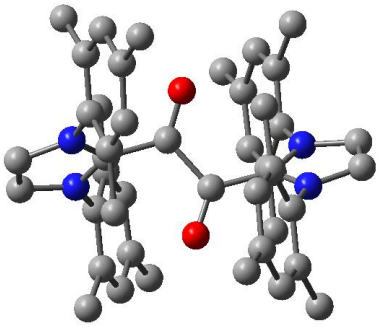

Charge = 2; Multiplicity = 1;

Atomic coordinates (Cartesian; in atomic unit)			
O	-0.1905393215	0.7807802425	1.4919768034
N	0.9120797792	2.2614998348	-1.480069668
N	-1.0021782435	2.7656224305	-0.5660578252
C	2.3696970861	0.9921641829	-2.9749774886
C	2.1818919444	1.6232572344	-1.7327683588
C	0.0341725764	0.6803383683	0.3145461917
C	-0.0055729663	1.8656302091	-0.588111266
C	3.617705931	0.4171417241	-3.2034364553
C	4.4231277602	1.1645734566	-1.0634889168
C	3.1853084843	1.7375931435	-0.7599728726
C	4.6581545826	0.4965140755	-2.2664915457
C	0.4967764107	3.4488348839	-2.0335305503
C	-2.2680060412	2.611016062	0.1179985062
C	-2.4569018524	3.2662171024	1.3420600272
C	-3.2486108548	1.8265403976	-0.5065625783
C	1.2993956902	0.9607124522	-4.0229600819
C	-0.711846264	3.7553211504	-1.4715922955
C	2.9708053602	2.4375601104	0.5499493392
C	5.9887796129	-0.118579606	-2.5650706671
C	-4.7186463735	2.3374603259	1.3799794883
C	-4.4746951925	1.7159902535	0.1506671472
C	-3.0000546394	1.0989043486	-1.7954031644
C	-3.6967847336	3.0997196251	1.9591253493
C	-1.3744916151	4.0981141047	1.9575642164
C	-6.0517900204	2.2069273578	2.0460163471
O	0.1089312485	-0.8331864975	-1.5302097138
N	1.0170639204	-2.2642671167	1.4757156374
N	-0.9054292239	-2.7647279118	0.582111558
C	2.4491673635	-0.9496199183	2.9548443589
C	2.2818954777	-1.6145222168	1.7262148096
C	0.150101779	-0.6979520629	-0.3378190213
C	0.0964265439	-1.8747341842	0.5878662317
C	3.6912650618	-0.3645041683	3.1884132268
C	4.5321601542	-1.164746048	1.0813661214
C	3.3017185358	-1.7505612928	0.7732437475
C	4.7466166812	-0.4654584004	2.2704223253
C	0.5978039607	-3.4453438174	2.0465731705
C	-2.1664023936	-2.6118756605	-0.111297417
C	-2.3294245736	-3.2451926897	-1.351483905
C	-3.1775218445	-1.875481881	0.5259932293
C	1.3596595661	-0.8936018763	3.9823514038
C	-0.6138246963	-3.7510035117	1.4956031062
C	3.1116601687	-2.4750150097	-0.5259109181
C	6.0731703516	0.1550037705	2.5757059491
C	-4.6153078403	-2.3789246373	-1.3887741769
C	-4.4007072622	-1.786215769	-0.1400828632
C	-2.9792602531	-1.1834784513	1.8423827416
C	-3.5682112462	-3.0982879139	-1.9765180602
C	-1.2255341934	-4.0453916547	-1.9712798036
C	-5.9353519944	-2.2295393728	-2.077383503
H	3.795304018	-0.0948135551	-4.1585638751
H	5.2377824306	1.2610670765	-0.3340385313
H	1.1087437445	3.9762087597	-2.7666175507
H	0.2934175732	0.7952331973	-3.5964951615
H	1.4910463578	0.158123986	-4.7547661652
H	1.2680299017	1.9084021574	-4.5960044332
H	-1.4014683607	4.5833720159	-1.6434178505
H	2.2787163279	3.2982036719	0.4728686729
H	3.9271593845	2.8243849583	0.9429350705
H	2.5705125485	1.7520872507	1.3266343693
H	5.8948363457	-1.2053634289	-2.7533502056
H	6.7072278195	0.0272778782	-1.7398068817
H	6.4351269684	0.3184518152	-3.4778617178
H	-5.2728811938	1.1285711101	-0.3231177166
H	-2.321545076	1.6411950935	-2.4820357818
H	-3.9470815226	0.9281702913	-2.3367142479
H	-2.562568527	0.0925644488	-1.6201584217
H	-3.8748613503	3.5907227908	2.9243945358
H	-0.4423356438	3.5165235333	2.0974608455
H	-1.6812894189	4.4776699335	2.9459809297
H	-1.1249112723	4.9792693068	1.3348442058
H	-6.7603135712	2.9636257063	1.6566934807
H	-5.9833481663	2.3597669412	3.1367556681
H	-6.5068558457	1.2172613798	1.8592909712
H	3.8518413516	0.1738810949	4.1319491494
H	5.3569520646	-1.2718303378	0.3642857759
H	1.2109080757	-3.9658633107	2.7835492802
H	0.362796275	-0.7231358841	3.5357274003
H	1.5471452714	-0.0855078227	4.7091306478
H	1.3063287607	-1.8346439314	4.5646469517
H	-1.3062848188	-4.5746203335	1.6766343942
H	2.3708499154	-3.2948792216	-0.4642658655
H	4.063431273	-2.922013509	-0.8623822922
H	2.7853670829	-1.7866731273	-1.3340531162
H	5.965192326	1.2185632762	2.8605454254
H	6.7668631486	0.0929569897	1.7191303306
H	6.559727333	-0.3498306988	3.4318388742
H	-5.2242220807	-1.2464010278	0.3476185428
H	-2.2200028706	-1.6654714763	2.4871289953
H	-3.9251997998	-1.1544149255	2.4118497102
H	-2.6708363829	-0.1261599197	1.7016172366
H	-3.7271801915	-3.5796658222	-2.9497900516
H	-0.313088532	-3.4354692238	-2.1173030739
H	-1.5263514806	-4.4358371801	-2.9572708869
H	-0.9463358607	-4.9169203196	-1.3476392023
H	-6.775766233	-2.3876930565	-1.3777875236
H	-6.0477950813	-2.9387657397	-2.9146013614
H	-6.051947409	-1.2088039895	-2.4929074661

2a^0 [E° = –2071.9229535; G° = –2071.189416] Def2-SV(P)

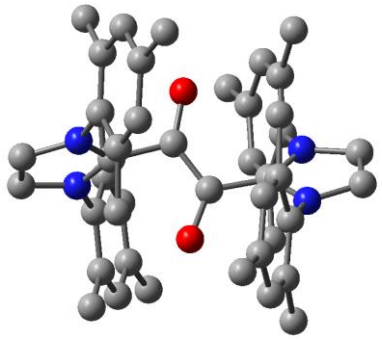

Charge = 0; Multiplicity = 1;

Atomic coordinates (Cartesian; in atomic unit)			
O	-0.3565716492	0.6753540214	1.5088442149
N	0.7784339796	2.0556572567	-1.6156509422
N	-0.9674782033	2.7239449448	-0.4720818403
C	2.3173636567	0.8067365072	-3.042092108
C	2.0660186046	1.4750089349	-1.8358291168
C	-0.0290519391	0.5534449037	0.2513507283
C	-0.0672165233	1.702971981	-0.6037858379
C	3.5980563428	0.2886231565	-3.2399066782
C	4.3094054117	1.0987808025	-1.0945217495
C	3.0429922362	1.6326274774	-0.8431719918
C	4.602834658	0.4174615871	-2.2774799527
C	0.388550892	3.2905173992	-2.1258781507
C	-2.2308545236	2.5810847928	0.1869854236
C	-2.4011427426	3.1021742002	1.4729521588
C	-3.2540457348	1.9117958489	-0.4989278674
C	1.2340536952	0.6319838923	-4.0579679945
C	-0.6937830387	3.6986537297	-1.4221654438
C	2.7510952995	2.3460021118	0.4435497533
C	5.9549157273	-0.1916102395	-2.5004420277
C	-4.7201148701	2.3436618746	1.4042661978
C	-4.4990682551	1.822394384	0.1265405906
C	-3.005598372	1.2744765507	-1.8333173156
C	-3.6609692226	2.9740795831	2.0618623747
C	-1.2389978875	3.6963463503	2.1998199386
C	-6.0585251864	2.1827053493	2.0614101756
O	0.463051785	-1.0178843695	-1.5664460774
N	1.0504618397	-2.260726747	1.4721766211
N	-0.9106105557	-2.6704114258	0.6548554073
C	2.4495383319	-0.8815578436	2.9134927224
C	2.3146095442	-1.6315135662	1.7353428179
C	0.2450448816	-0.679503404	-0.3618098371
C	0.1215176715	-1.8101130599	0.6133145717
C	3.6908508808	-0.2918672428	3.1536246989
C	4.577596238	-1.2006168012	1.1129491433
C	3.3534370182	-1.8041752968	0.8134102618
C	4.7620067089	-0.4374848697	2.2663862028
C	0.5950960199	-3.4221242818	2.076175816
C	-2.147417588	-2.5003685336	-0.0561917415
C	-2.2737755741	-3.071728524	-1.3272704581
C	-3.1604488318	-1.7471131621	0.5555833017
C	1.2894336968	-0.6863016887	3.8384863611
C	-0.6366753095	-3.6770140169	1.5656514964
C	3.1522008787	-2.5644237818	-0.4602290205
C	6.0664712394	0.2518227943	2.532223822
C	-4.5363861836	-2.1630475915	-1.4213264428
C	-4.3563140722	-1.606898714	-0.1516640957
C	-2.9493977127	-1.0888316186	1.8811667764
C	-3.4881598927	-2.8884056761	-1.9933575615
C	-1.1283301435	-3.8044317046	-1.9527994479
C	-5.8216949116	-1.945762211	-2.1620171725
H	3.8145079137	-0.2418643412	-4.1778222649
H	5.0961095088	1.2268483152	-0.3379517608
H	0.954797738	3.7707254169	-2.9241025326
H	0.395876287	0.0817307208	-3.5880763061
H	1.5956433725	0.0571238309	-4.9286100992
H	0.8417459134	1.5980126865	-4.4318417726
H	-1.3170405504	4.5892754852	-1.5073848646
H	2.2172685292	3.302688649	0.2739621518
H	3.6857980605	2.5699396369	0.9890619915
H	2.1046624953	1.7403999401	1.1117797274
H	5.9311338802	-1.2889257872	-2.3403345902
H	6.7104380202	0.2242944888	-1.808730578
H	6.3132595244	-0.0301830604	-3.534317946
H	-5.3242057145	1.3248398767	-0.4036564964
H	-2.4956184191	1.9573772044	-2.5408789305
H	-3.9523916057	0.9460218843	-2.2986912138
H	-2.3547273727	0.3802565358	-1.7316426341
H	-3.815198605	3.3732443564	3.0738010255
H	-0.4783810322	2.8974063015	2.3230120542
H	-1.5348915004	4.0794887079	3.1921764981
H	-0.7684694142	4.5244108665	1.6347610854
H	-6.8856281869	2.4190276257	1.365996534
H	-6.1620032565	2.8327867546	2.9484031733
H	-6.213967806	1.1381348734	2.3998272023
H	3.821896293	0.3096983433	4.0638176771
H	5.4112147866	-1.3229326403	0.4076412658
H	1.2025990483	-3.9520892252	2.8096442288
H	0.4575184746	-0.2160588661	3.2715099548
H	1.5668559677	-0.0313012093	4.6827108374
H	0.9246353549	-1.6428562594	4.2622462072
H	-1.3546541632	-4.4739856189	1.758909044
H	2.6639750616	-3.5441720812	-0.2863874555
H	4.1162548079	-2.7475910005	-0.9672176599
H	2.4916409332	-2.0009161326	-1.1545008413
H	5.9891596649	1.3391002819	2.32947106
H	6.8768231491	-0.1446185948	1.8939775335
H	6.3786997022	0.1468230313	3.5879763942
H	-5.1744241243	-1.0370482499	0.310706951
H	-2.6328972503	-1.8143209777	2.6577022418
H	-3.877653251	-0.5997578012	2.2280962602
H	-2.1407257317	-0.3175135354	1.8206223061
H	-3.6139881665	-3.3242069487	-2.9937481227
H	-0.2763621875	-3.1033826279	-2.0786415154
H	-1.407210772	-4.2107449086	-2.9404746496
H	-0.7814387566	-4.647997122	-1.3237614722
H	-6.6977839157	-2.0500834263	-1.4954176321

H	-5.9402574291	-2.6571233244	-2.9986422583	H	-5.8657205903	-0.9243791383	-2.5910705133

Cl_2 [E° = –920.0361141; G° = –920.056732; G°(THF) = –920.0599524; G°(MeCN) = –920.059756] Def2-SV(P)

Charge = 0; Multiplicity = 1;

Atomic coordinates (Cartesian; in atomic unit)			
Cl	-0.2453610738	0.35539215	0.0
Cl	-2.2738546062	0.35539215	0.0

$2a^{2+}$ • Cl^- [E° = –2531.7803883; G° = –2531.050256; G°(THF) = –2531.1382281; G°(MeCN) = –2531.1482169] Def2-SV(P)

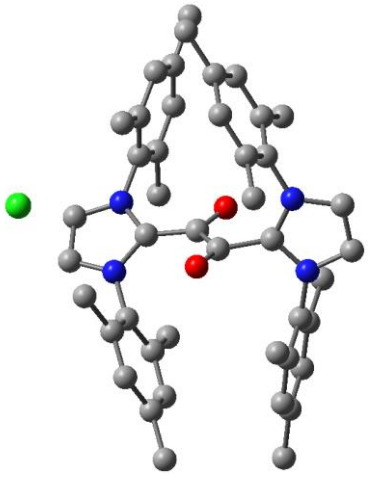

Charge = 1; Multiplicity = 1;

Atomic coordinates (Cartesian; in atomic unit)			
O	0.9268901987	1.2766962929	1.1411890864
N	0.4105269457	-1.7430146401	1.8834443309
N	-1.4601804943	-2.2356057109	0.834314626
O	-0.6436520587	-0.5404002886	-1.3547868724
N	1.6704353021	1.8511214516	-1.9624157885
N	-0.2978101819	2.6547009038	-1.520720207
C	0.6185821945	1.7598039008	-1.1470612262
C	-0.3876233945	-1.3782494808	0.8251346579
C	2.0920753279	-0.4985590083	3.1689052936
C	1.7785322502	-1.3373707601	2.088444782
C	-2.6255704117	-2.1303964816	-0.0143603412
C	-1.3743223392	-3.0512797378	1.8968222697
C	-0.1939977357	-2.7355190415	2.5742235465
C	0.5312229365	0.8705786349	0.0790209629
C	-2.7081338861	-2.9749085895	-1.1272722754
C	-3.6044145759	-1.1831104956	0.3108786723
C	3.4322989517	-0.1438364909	3.3221615546
C	2.8444203954	1.0142771513	-1.9117462113
C	2.7396851193	-1.8339037309	1.1978846714
C	-1.6270122195	3.6702631378	0.2523047163
C	-1.5808155075	2.8433828403	-0.8852699482
C	-0.1717730264	-0.4231131616	-0.2175606746
C	2.9119081289	-0.0670849658	-2.8083092988
C	1.4178044432	2.8415698743	-2.8957648002
C	-2.863294224	3.8312635888	0.8709903215
C	3.8684645987	1.3332070606	-1.0115482266
C	4.067036623	-1.4522278548	1.4104296221
C	-2.7105293916	2.2211069047	-1.4319712463
C	0.1851130113	3.3455149696	-2.6171547668
C	-3.8439156725	-2.8684800943	-1.9282041008
C	-4.7233691972	-1.1267094106	-0.525368182
C	-4.8663313227	-1.9579846577	-1.6389427964
C	-3.453587506	-0.2398658517	1.4642916352
C	5.1206813112	-0.5705205725	-1.895023453
C	-3.9256777869	2.43722719	-0.773492119
C	2.3811450264	-2.7354936043	0.0524437533
C	5.0043106386	0.5190625306	-1.0320490141
C	1.041341531	0.0120002724	4.0998818276
C	-6.0969808777	-1.8917127634	-2.4898667658
C	-4.0233318366	3.2206361394	0.3755445735
C	4.0626935668	-0.8504226068	-2.7694662984
C	4.4313866705	-0.6050316562	2.4577301328
C	1.7944806407	-0.3630967474	-3.7622825745
C	-1.5971634101	-3.9213936275	-1.4604539551
C	-2.6734209928	1.3330601984	-2.6375846692
C	-0.3969286754	4.3530478972	0.7702443087
C	-5.334794207	3.4199940201	1.0688731221
C	3.7626071674	2.4570141548	-0.0277397167
C	6.3434157665	-1.4346736332	-1.8959882956
C	5.8563945087	-0.1892675853	2.6600499226
H	-2.1494808328	-3.7760840442	2.1434004486
H	0.3064018219	-3.249621887	3.3937549733
H	3.7073740847	0.5149183306	4.1569214253

H	2.1487772185	3.0885818698	-3.6659337286	H	-0.6512634267	-3.3700676375	-1.6328325385
H	-2.928642527	4.461806477	1.767454346	H	-1.8248894024	-4.4952017493	-2.3744529833
H	4.8427304329	-1.8470584136	0.7409777887	H	-1.4079498094	-4.6514517049	-0.6496130622
H	-0.404310493	4.1316623993	-3.0896900355	H	-1.7488948135	1.4353671992	-3.2326681621
H	-3.9341779026	-3.5183828588	-2.8085985385	H	-3.5356205538	1.5426985227	-3.2965469275
H	-5.5203793705	-0.4096620228	-0.283849915	H	-2.7368217864	0.269506405	-2.3334061051
H	-3.0729629272	-0.7276629651	2.3848420096	H	0.3521389044	3.6287002676	1.1466823983
H	-4.4223922108	0.2320219901	1.7060521048	H	-0.6469550458	5.0310072468	1.603188454
H	-2.7494128517	0.5839624745	1.2168249708	H	0.0975842452	4.9594099743	-0.0139553703
H	-4.8287036032	1.9645789616	-1.1833010532	H	-5.2397674044	3.2608843704	2.1588820144
H	1.5824346859	-3.4573280912	0.3127508357	H	-6.109694745	2.7320876599	0.687368759
H	3.2608475797	-3.31592135	-0.2781226899	H	-5.7081256645	4.4525596676	0.9284954603
H	2.02656009	-2.1631179646	-0.8306466067	H	3.1116392042	3.2801804231	-0.3774413737
H	5.8260781599	0.7485337638	-0.3399874265	H	4.7578202417	2.8828813573	0.1893872352
H	0.2233788534	0.511499763	3.547455365	H	3.3422141308	2.0941573745	0.9326174208
H	1.4707462606	0.732589268	4.8163003922	H	7.0311343564	-1.178517211	-1.0710889902
H	0.5468586839	-0.7953433985	4.672907653	H	6.9065250817	-1.3296682483	-2.8429722185
H	-5.8927901511	-2.2013974464	-3.5300335292	H	6.0781569337	-2.5051678183	-1.8038757158
H	-6.5266879905	-0.87395932	-2.5086078675	H	5.9848635179	0.8980216083	2.4903233404
H	-6.8840402925	-2.5661977208	-2.099836506	H	6.541904199	-0.7213577306	1.9764887115
H	4.1420439965	-1.7074426958	-3.4519208311	H	6.1923355842	-0.386847377	3.694899357
H	0.8122972892	-0.4057331127	-3.2515279531	Cl	-1.8913614512	-1.8966666332	4.3199934294
H	1.9580076617	-1.3297162821	-4.2680782492				
H	1.717313715	0.4068104452	-4.5553250817				

Molecular orbitals

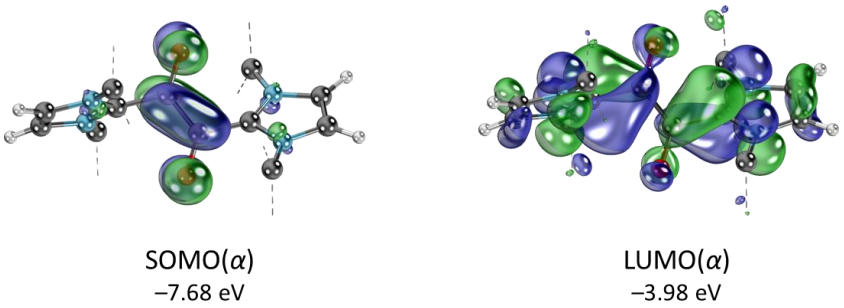

Figure S5. SOMO and LUMO of $\mathbf{2a}^{\bullet+}$.

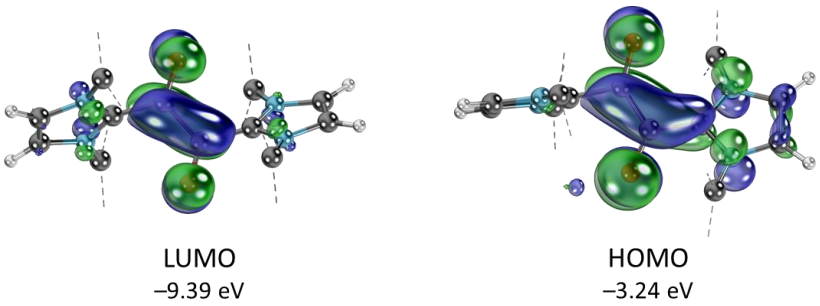

Figure S6. LUMO of $\mathbf{2a}^{2+}$ (left) and HOMO of $\mathbf{2a}^{0}$ (right).

Wiberg bond index

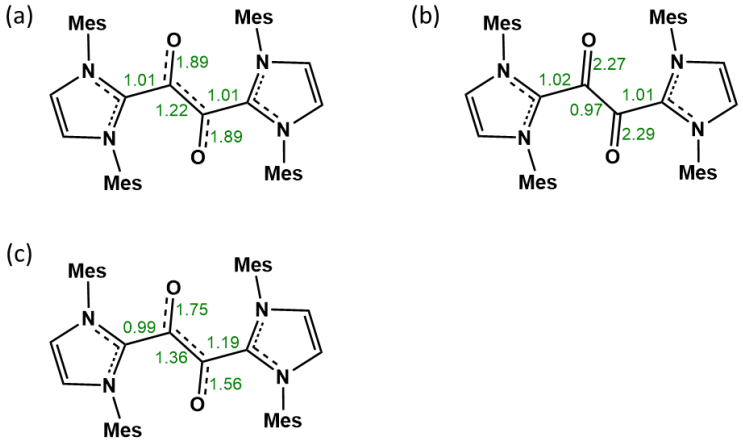

Figure S7. Selected Wiberg bond indices for (a) $\mathbf{2a}^{\bullet+}$, (b) $\mathbf{2a}^{2+}$, and (c) $\mathbf{2a}^{0}$.

X-ray Crystallography

CCDC 2011174-2011177 and 2050164 contains the supplementary crystallographic data for [**2a**$^{\bullet+}$][BF_4^-], [**2b**$^{\bullet+}$][BF_4^-], [**2a**$^{2+}$][BF_4^-]$_2$, [**2a**$^{\bullet+}$][Cl^-], and **2a**^{0} respectively. These data can be obtained free of charge *via* https://www.ccdc.cam.ac.uk/

General information

A suitable crystal was coated with paratone-*N* oil and the diffraction data measured either with a graphite-monochromated Mo Kα radiation source on a Bruker Venture CMOS diffractometer or a synchrotron radiation on a 2D beamline at the Pohang Accelerator Laboratory, Korea. Using Olex2,[10] The structure was solved by ShelXT[11] using intrinsic phasing and refined by ShelXL[12] using least squares minimization. All the non-hydrogen atoms were refined anisotropically. All hydrogen atoms were added to their geometrically ideal positions. Solvent mask[13] was used to exclude solvent and some anion molecules during the refinement of [**2a**$^{\bullet+}$][Cl^-] (Grid = 0.25 Å, Solvent R = 1.2 Å).

	[**2a**$^{\bullet+}$][BF_4^-]	[**2b**$^{\bullet+}$][BF_4^-]	[**2a**$^{2+}$][BF_4^-]$_2$	[**2a**$^{\bullet+}$][Cl^-]	**2a**^{0}
Empirical formula	$C_{44}H_{48}BF_4N_4O_2$	$C_{56}H_{72}BF_4N_4O_2$	$C_{46}H_{52}B_2Cl_4F_8N_4O_2$	$C_{44}H_{48}Cl_{0.67}N_4O_2$	$C_{44}H_{48}N_4O_2$
Formula weight	751.67	919.98	1008.33	688.49	664.86
Temperature/K	100	100	100.0	293(2)	100
Crystal system	monoclinic	monoclinic	triclinic	trigonal	orthorhombic
Space group	I2/a	$P2_1/n$	P-1	P-3c1	Pbca
a/Å	15.4206(9)	14.6496(10)	11.438(7)	20.645(3)	17.113(6)
b/Å	16.1466(10)	22.7009(14)	11.822(6)	20.645(3)	18.399(6)
c/Å	17.1235(13)	16.5084(11)	20.180(12)	16.312(3)	22.754(6)
α/°	90	90	88.103(15)	90	90
β/°	108.011(4)	92.586(2)	84.082(18)	90	90
γ/°	90	90	69.483(14)	120	90
Volume/Å^3	4054.7(5)	5484.4(6)	2542(3)	6021(2)	7164(4)
Z	4	4	2	6	8
ρ_{calc}g/cm^3	1.231	1.114	1.317	1.139	1.233
μ/mm^{-1}	0.088	0.076	0.302	0.111	0.076
F(000)	1588.0	1972.0	1044.0	2204.0	2848.0
Crystal size/mm^3	0.15 × 0.08 × 0.05	0.3 × 0.05 × 0.05	0.3 × 0.15 × 0.03	0.08 × 0.04 × 0.03	0.06 × 0.05 × 0.02
Radiation	MoKα (λ = 0.71073)	MoKα (λ = 0.71073)	MoKα (λ = 0.71073)	synchrotron (λ = 0.700)	MoKα (λ = 0.71073)
2Θ range for data collection/°	5.046 to 52.178	5.11 to 50.066	4.28 to 50.054	3.886 to 59.632	3.58 to 50.052
Index ranges	-19 ≤ h ≤ 19 -19 ≤ k ≤ 19 -21 ≤ l ≤ 21	-17 ≤ h ≤ 17 -27 ≤ k ≤ 27 -19 ≤ l ≤ 19	-13 ≤ h ≤ 13 -14 ≤ k ≤ 13 -24 ≤ l ≤ 24	-29 ≤ h ≤ 29 -24 ≤ k ≤ 24 -20 ≤ l ≤ 17	-20 ≤ h ≤ 20 -21 ≤ k ≤ 21 -27 ≤ l ≤ 27
Reflections collected	33904	84766	31408	15034	153360
Independent reflections	3995 [R_{int} = 0.0645, R_{sigma} = 0.0298]	9692 [R_{int} = 0.1212, R_{sigma} = 0.0610]	8929 [R_{int} = 0.0963, R_{sigma} = 0.0907]	4642 [R_{int} = 0.0421, R_{sigma} = 0.0458]	6320 [R_{int} = 0.1383, R_{sigma} = 0.0527]
Data/restraints /parameters	3995/0/255	9692/60/648	8929/78/644	4642/0/235	6320/0/463
Goodness-of-fit on F^2	1.071	1.026	1.020	1.103	1.036
Final R indexes [I>=2σ (I)]	R_1 = 0.0561 wR_2 = 0.1386	R_1 = 0.0898 wR_2 = 0.2465	R_1 = 0.0847 wR_2 = 0.1956	R_1 = 0.0596 wR_2 = 0.1617	R_1 = 0.0545 wR_2 = 0.1250
Final R indexes [all data]	R_1 = 0.0829 wR_2 = 0.1588	R_1 = 0.1618 wR_2 = 0.3018	R_1 = 0.1496 wR_2 = 0.2372	R_1 = 0.0815 wR_2 = 0.1724	R_1 = 0.0907 wR_2 = 0.1457
Largest diff. peak /hole / e Å^{-3}	0.22/-0.23	0.50/-0.45	0.45/-0.43	0.36/-0.62	0.68/-0.29

Structural data

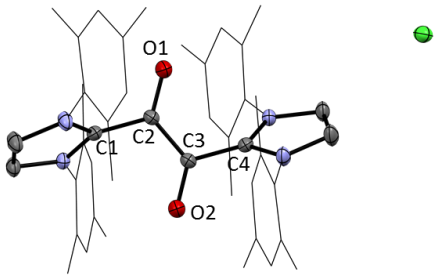

[**2a**$^{\bullet+}$][Cl$^-$]

Table S1. Selected bond lengths (Å) and angles (°).

Bond length (Å)	C1–C2	C2–C3	C3–C4	O1–C2	O2–C3
[**2a**$^{\bullet+}$][BF_4^-]	1.495(3)	1.409(2)	1.495(3)	1.246(3)	1.246(3)
[**2b**$^{\bullet+}$][BF_4^-]	1.497(5)	1.407(4)	1.499(5)	1.247(4)	1.251(4)
[**2a**$^{\bullet+}$][Cl$^-$]	1.498(2)	1.433(3)	1.498(2)	1.249(3)	1.249(3)
[**2a**$^{2+}$][BF_4^-]$_2$	1.488(5)	1.535(5)	1.480(5)	1.190(5)	1.202(5)
2a^0	1.510(4)	1.349(4)	1.477(4)	1.300(3)	1.311(3)

Bond angle (°)	C1–C2–O1	O1–C2–C3	C1–C2–C3	C2–C3–O2	C2–C3–C4	O2–C3–C4
[**2a**$^{\bullet+}$][BF_4^-]	118.2(2)	125.1(2)	116.5(2)	125.1(2)	116.5(2)	118.2(2)
[**2b**$^{\bullet+}$][BF_4^-]	118.2(3)	123.5(3)	118.3(3)	123.5(3)	117.8(3)	118.5(3)
[**2a**$^{\bullet+}$][Cl$^-$]	119.3(2)	125.2(2)	115.3(2)	125.2(2)	115.3(2)	119.3(2)
[**2a**$^{2+}$][BF_4^-]$_2$	121.3(4)	120.7(4)	117.3(3)	119.0(4)	119.2(3)	121.1(4)
2a^0	117.1(2)	131.8(3)	110.9(2)	128.8(3)	112.8(2)	118.2(2)

Torsion angle (°)	NHC–C1–C2–O1	O1–C2–C3–O2	O2–C3–C4–NHC2
[**2a**$^{\bullet+}$][BF_4^-]	53.0(3)	172.8(2)	53.0(3)
[**2b**$^{\bullet+}$][BF_4^-]	66.9(5)	179.5(4)	60.0(5)
[**2a**$^{\bullet+}$][Cl$^-$]	57.8(3)	171.0(2)	57.8(3)
[**2a**$^{2+}$][BF_4^-]$_2$	44.9(6)	156.8(4)	36.6(6)
2a^0	54.7(3)	170.0(3)	42.7(4)

The thermal ellipsoids are set at a 50% probability level. Hydrogens, solvents, disorders were omitted for clarity.

Table S2. Metric comparison between DFT optimized and X-ray determined structures.

Bond length (Å)	C1–C2	C2–C3	C3–C4	O1–C2	O2–C3
[**2a**$^{\bullet+}$][BF_4^-] (X-ray)	1.495(3)	1.409(2)	1.495(3)	1.246(3)	1.246(3)
2a$^{\bullet+}$ (DFT)	1.493	1.433	1.491	1.248	1.249
[**2a**$^{2+}$][BF_4^-]$_2$(X-ray)	1.488(5)	1.535(5)	1.480(5)	1.190(5)	1.202(5)
2a^{2+} (DFT)	1.498	1.529	1.490	1.201	1.203
2a^{0} (X-ray)	1.510(4)	1.349(4)	1.477(4)	1.300(3)	1.311(3)
2a^{0} (DFT)	1.498	1.404	1.433	1.270	1.305

Bond angle (°)	C1–C2–O1	O1–C2–C3	C1–C2–C3	C2–C3–O2	C2–C3–C4	O2–C3–C4
[**2a**$^{\bullet+}$][BF_4^-] (X-ray)	118.2(2)	125.1(2)	116.5(2)	125.1(2)	116.5(2)	118.2(2)
2a$^{\bullet+}$ (DFT)	118.5	125.8	115.6	125.5	115.8	118.5
[**2a**$^{2+}$][BF_4^-]$_2$(X-ray)	121.3(4)	120.7(4)	117.3(3)	119.0(4)	119.2(3)	121.1(4)
2a^{2+} (DFT)	121.6	121.5	116.2	120.5	117.4	121.4
2a^{0} (X-ray)	117.1(2)	131.8(3)	110.9(2)	128.8(3)	112.8(2)	118.2(2)
2a^{0} (DFT)	115.5	133.0	111.2	123.5	116.7	119.6

Torsion angle (°)	NHC–C1–C2–O1	O1–C2–C3–O2	O2–C3–C4–NHC2
[**2a**$^{\bullet+}$][BF_4^-] (X-ray)	53.0(3)	172.8(2)	53.0(3)
2a$^{\bullet+}$ (DFT)	57.5	172.7	55.1
[**2a**$^{2+}$][BF_4^-]$_2$(X-ray)	44.9(6)	156.8(4)	36.6(6)
2a^{2+} (DFT)	56.8	165.1	46.5
2a^{0} (X-ray)	54.7(3)	170.0(3)	42.7(4)
2a^{0} (DFT)	70.1	173.0	33.2

DFT calculation at M06/Def2-SV(P).

EPR

General information

EPR spectra were recorded on a Bruker X-band A200 spectrometer using dry dichloromethane solutions. Spectra processing and simulation were performed with Bruker WIN-EPR and EasySpin associated with DFT calculations.[14] Isotropic hyperfine coupling constants were initially computed using gaussian09 with M06/Def2-SV(P) basis sets, and then rescaled to fit the experimental data.

EPR spectra

(a)

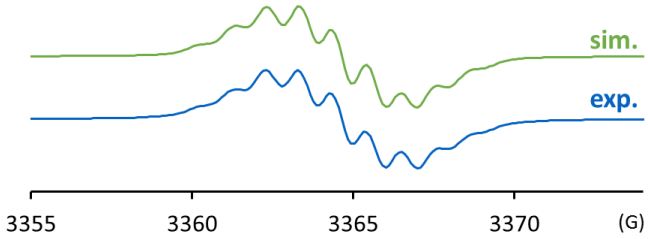

(b)

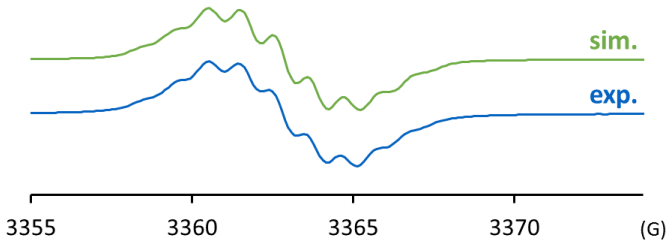

Figure S8. (a) Experimental (bottom, blue) and simulated (top, green) EPR spectra of **[2a$^{\bullet+}$][BF$_4^-$]** at microwave frequency = 9.4467 GHz. Simulated with the following parameters: g_{iso} = 2.0060; hyperfine coupling constants: a(^{14}N) = 3.0, 3.0, 2.6, 2.6 MHz; Gaussian line width = 0.04 mT; Lorentzian line width = 0.04 mT. (b) Experimental (bottom, blue) and simulated (top, green) EPR spectra of **[2b$^{\bullet+}$][BF$_4^-$]** at microwave frequency = 9.4413 GHz. Simulated with the following parameters: g_{iso} = 2.0059; hyperfine coupling constants: a(^{14}N) = 3.0, 3.0, 2.6, 2.6 MHz; Gaussian line width = 0.05 mT; Lorentzian line width = 0.04 mT.

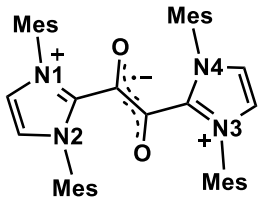

hfcc	N1	N2	N3	N4
Exp	2.6	3.0	2.6	3.0
M06/6-31G(d,p)	2.8	3.1	2.8	3.0
M06/Def2SV(P)	3.7	4.5	3.6	4.4

Figure S9. Comparison of hyperfine coupling constants for **[2a$^{\bullet+}$][BF$_4^-$]** from experiment and DFT calculations at M06/6-31G(d,p) or M06/Def2-SV(P).

Thermal stability

a)

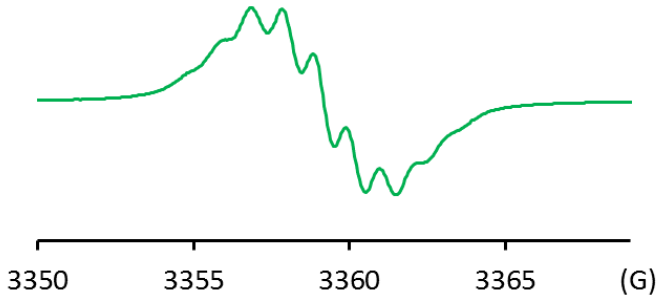

b)

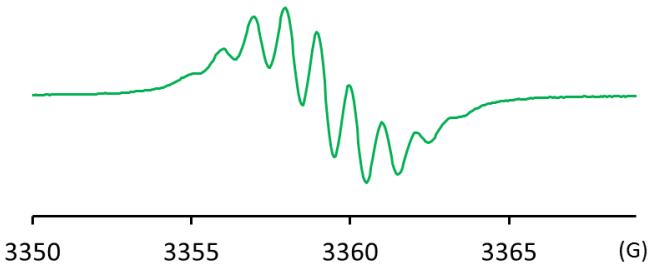

Figure S10. (a) Experimental EPR spectra of **[2a$^{\bullet+}$][Cl$^-$]** after heating for 7 days at 120°C under air (in solid state) at microwave frequency = 9.4328 GHz (measured with dichloromethane solution). (b) Experimental EPR spectra of **[2a$^{\bullet+}$][Cl$^-$]** after heating for 6 hours at 200°C under air (in solid state) at microwave frequency = 9.4337 GHz (measured with dichloromethane solution).

Cyclic Voltammetry

General information

Cyclic voltammograms were recorded at room temperature with either a BioLogic SP-300 potentiostat or Princeton Applied Research (PAR) VersaSTAT 3 potentiostat. The working electrode was a glassy carbon disk (area = 0.02 cm^2), the reference electrode was Ag/AgCl (saturated), and the counter electrode was a platinum wire.

Cyclic voltammograms

(a)

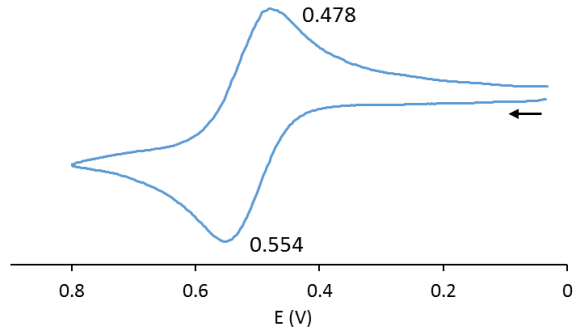

(b)

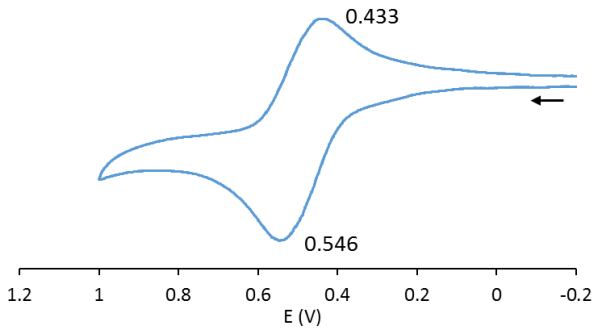

Figure S11. (a) Cyclic voltammogram of **[2a$^{\bullet+}$][BF_4^-]** (3.1 mM) in dry and degassed acetonitrile with Bu_4NPF_6 (0.1 M) as the supporting electrolyte (scan rate = 0.1 V/s). The cyclic voltammogram showed reversible one-electron redox potential at $E_{1/2}$ = 0.516 V versus Ag/AgCl (saturated) electrode, which corresponds to **2a**$^{2+}$ + e^- ⇄ **2a**$^{\bullet+}$. (b) Cyclic voltammogram of **[2b$^{\bullet+}$][BF_4^-]** (2.9 mM) in dry and degassed acetonitrile with Bu_4NPF_6 (0.1 M) as the supporting electrolyte (scan rate = 0.1 V/s). The cyclic voltammogram showed reversible one-electron redox potential at $E_{1/2}$ = 0.490 V versus Ag/AgCl (saturated) electrode, which corresponds to **2b**$^{2+}$ + e^- ⇄ **2b**$^{\bullet+}$.

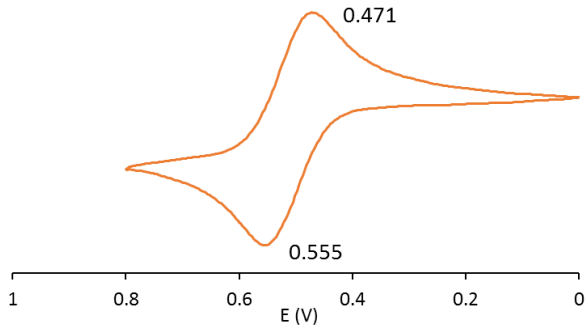

Figure S12. Cyclic voltammogram of **[2a^{2+}][BF$_4^-$]$_2$** (2.6 mM) in dry and degassed acetonitrile with Bu_4NPF_6 (0.1 M) as the supporting electrolyte (scan rate = 0.1 V/s). The cyclic voltammogram was identical to that of **[2a$^{\bullet+}$][BF$_4^-$]**, showing reversible one-electron redox potential at $E_{1/2}$ = 0.513 V versus Ag/AgCl (saturated) electrode, which corresponds to **2a^{2+}** + e^- ⇄ **2a$^{\bullet+}$**.

(a)

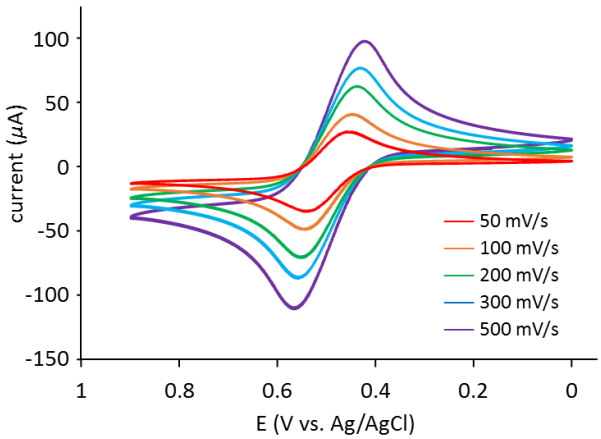

(b)

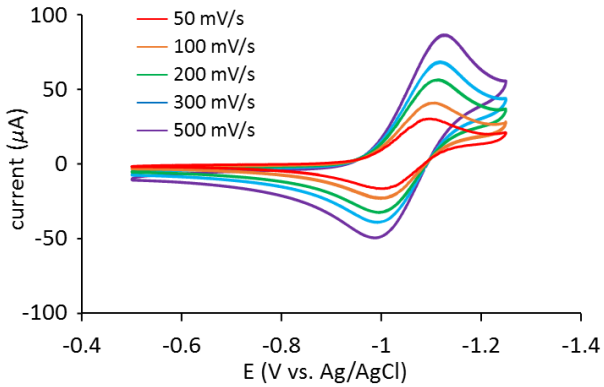

Figure S13. Cyclic voltammogram of **[2a$^{\bullet+}$][BF$_4^-$]** (4.5 mM) in dry and degassed acetonitrile with Bu_4NPF_6 (0.1 M) as the supporting electrolyte under various scan rates. (a) Oxidative potential scan showing reversible one-electron redox potential at $E_{1/2}$ = 0.498 V versus Ag/AgCl (saturated) electrode, which corresponds to **2a^{2+}** + e^- ⇄ **2a$^{\bullet+}$**. (a) Reductive potential scan showing reversible one-electron redox potential at $E_{1/2}$ = –1.051 V versus Ag/AgCl (saturated) electrode, which

corresponds to $\mathbf{2a}^{\bullet+} + e^- \rightleftarrows \mathbf{2a}^0$.

(a)

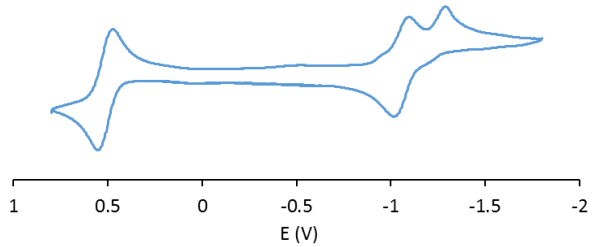

(b)

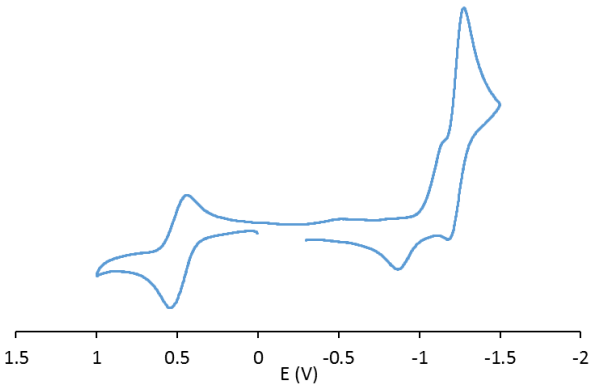

Figure S14. Extended range scan of (a) $\mathbf{[2a^{2+}][BF_4^-]_2}$ (2.6 mM) and (b) $\mathbf{[2b^{\bullet+}][BF_4^-]}$ (2.9 mM) in dry and degassed acetonitrile (0.1 M Bu_4NPF_6; scan rate = 0.1 V/s). Potential versus Ag/AgCl (saturated) electrode.

UV-Vis Spectroscopy

General information

The UV-vis spectra were recorded at room temperature with Cary 6000i UV-Vis-NIR (Agilent Technologies) with quartz UV cell.

Experimental and simulated UV-Vis spectra

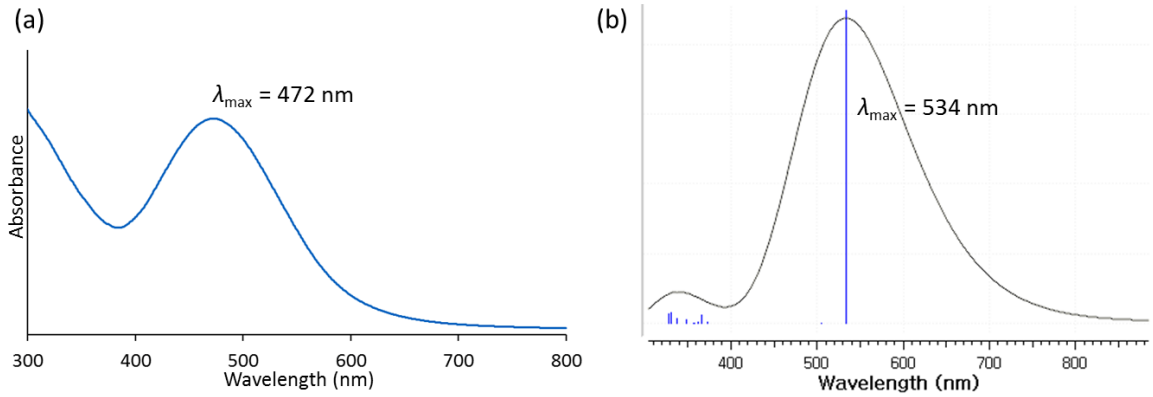

Figure S15. (a) UV-vis absorption of **[2a$^{\bullet+}$][Cl^{-}]** in distilled water (path length = 10 mm). (b) Simulated UV-vis absorption from DFT calculation at M06/Def2-SV(P).

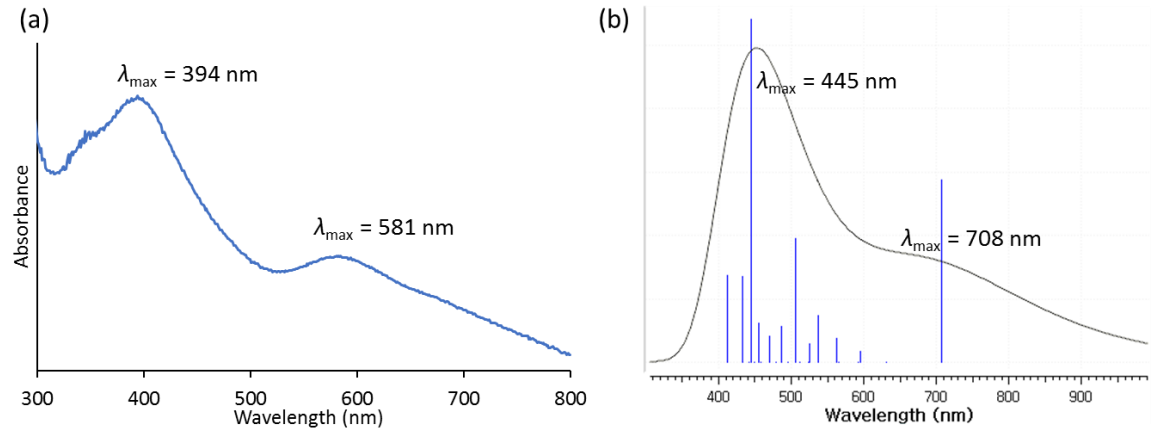

Figure S16. (a) UV-vis absorption of **2a^{0}** in dry benzene (path length = 1 mm). (b) Simulated UV-vis absorption from DFT calculation at M06/Def2-SV(P).

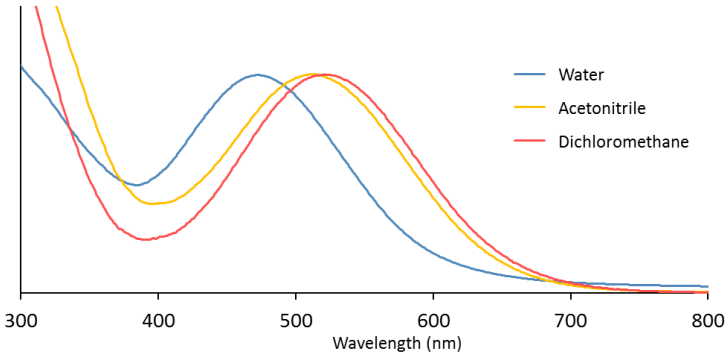

Figure S17. Comparison of UV-vis spectra of **[2a$^{\bullet+}$][Cl$^-$]** in distilled water (blue; λ_{max} = 472 nm), acetonitrile (yellow; λ_{max} = 510 nm), and dichloromethane (red; λ_{max} = 521 nm).

Stability

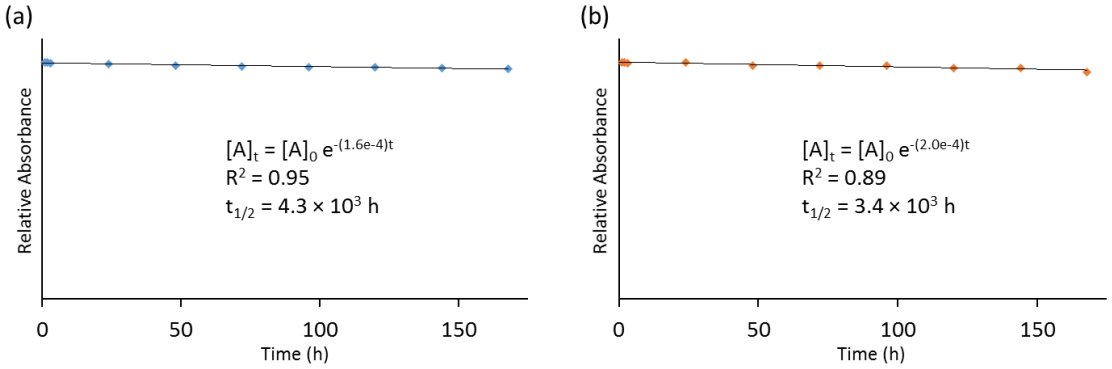

Figure S18. Decay of **[2a$^{\bullet+}$][Cl$^-$]** (0.16 mM; peak height at λ_{max} = 472 nm) in 0.1 M potassium phosphate buffer (pH 7.4) (a) without sodium ascorbate and (b) with excess sodium ascorbate (4 mM) monitored by UV-vis. Half-life was calculated by assuming 1st order kinetics.

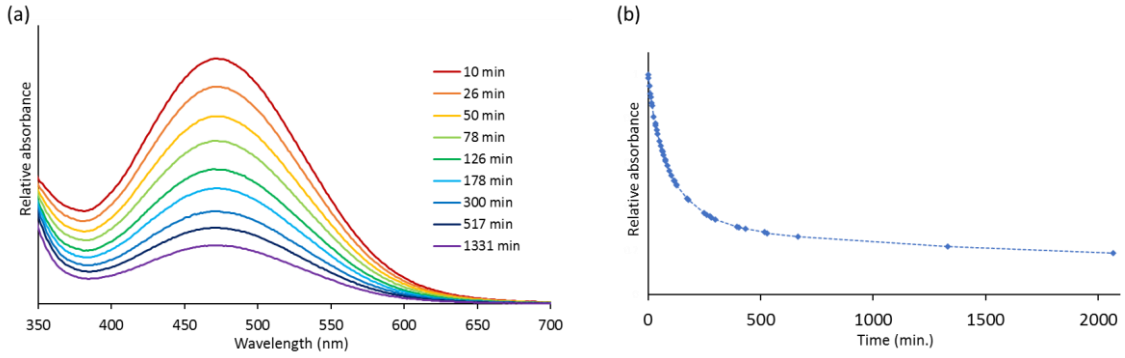

Figure S19. Decay of **[2a$^{\bullet+}$][Cl$^-$]** (0.16 mM; λ_{max} = 472 nm) in 0.1 M sulfuric acid. (a) Selected spectra. (b) Absorbance at 472 nm for 2000 minutes.

IR Spectroscopy

General information

The IR spectra were recorded at room temperature with Cary 600 FTIR Spectrometer (Agilent Technologies) equipped with GladiATR (PIKE technologies).

Experimental spectra

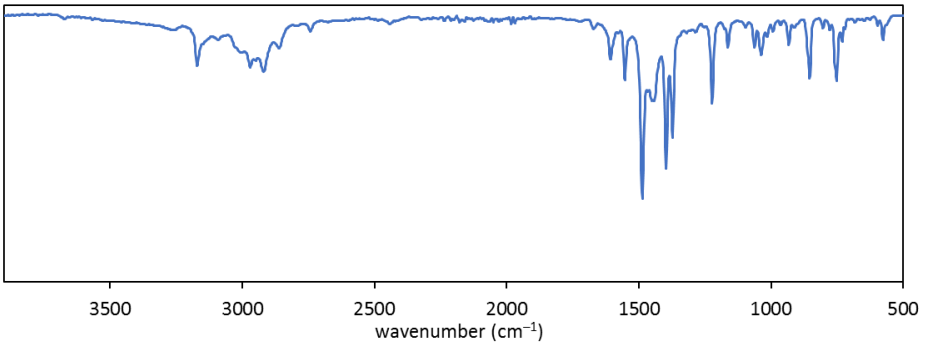

Figure S20. IR spectrum of **[2a$^{\bullet+}$][Cl$^-$]**.

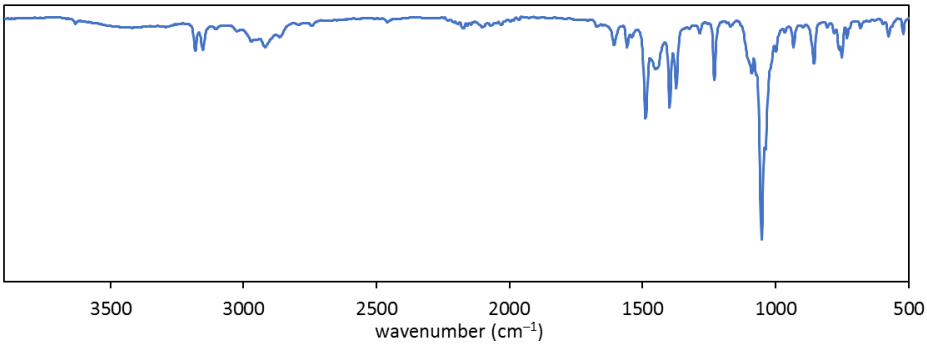

Figure S21. IR spectrum of **[2a$^{\bullet+}$][BF$_4^-$]**.

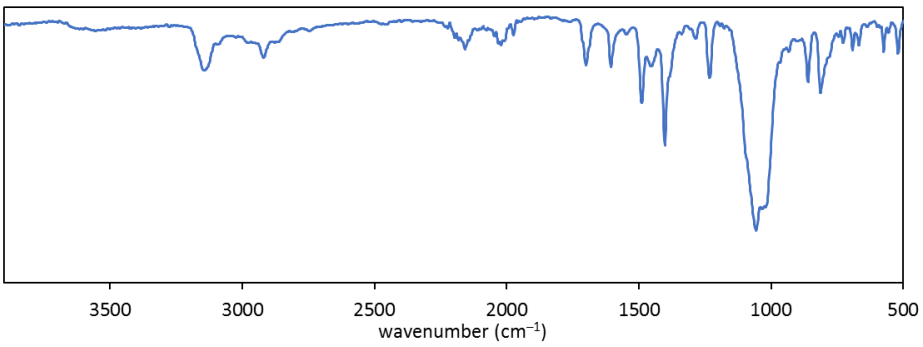

Figure S22. IR spectrum of **[2a^{2+}][BF$_4^-$]$_2$**.

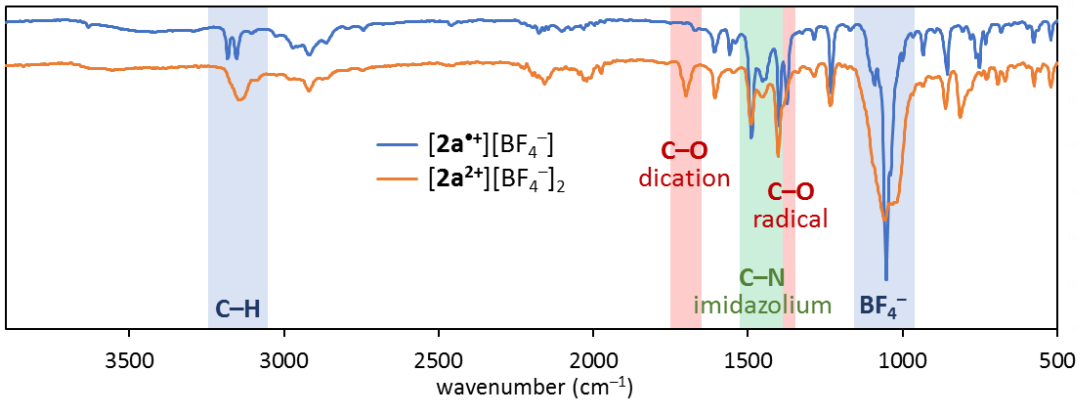

Figure S23. Comparison and signal assignment.

NMR

General information

^{1}H NMR spectra, proton decoupled ^{13}C NMR spectra (^{13}C{^{1}H}), and proton decoupled ^{19}F NMR spectra (^{19}F{^{1}H}) were recorded using either a Bruker DRX 500 spectrometer, Bruker AVANCE III 300 spectrometer, or AVANCE III HD 850 spectrometer. Chemical shifts of ^{1}H and ^{13}C acquisitions were referenced to the residual solvent peaks (^{1}H: CD_3CN, δ = 1.94 ppm; C_6D_6, δ = 7.16 ppm; ^{13}C: CD_3CN, δ = 118.26 ppm; C_6D_6, δ = 128.06 ppm).[15]

NMR spectra

^{1}H, ^{13}C, ^{19}F NMR spectra of $[2a^{2+}][BF_4^-]_2$

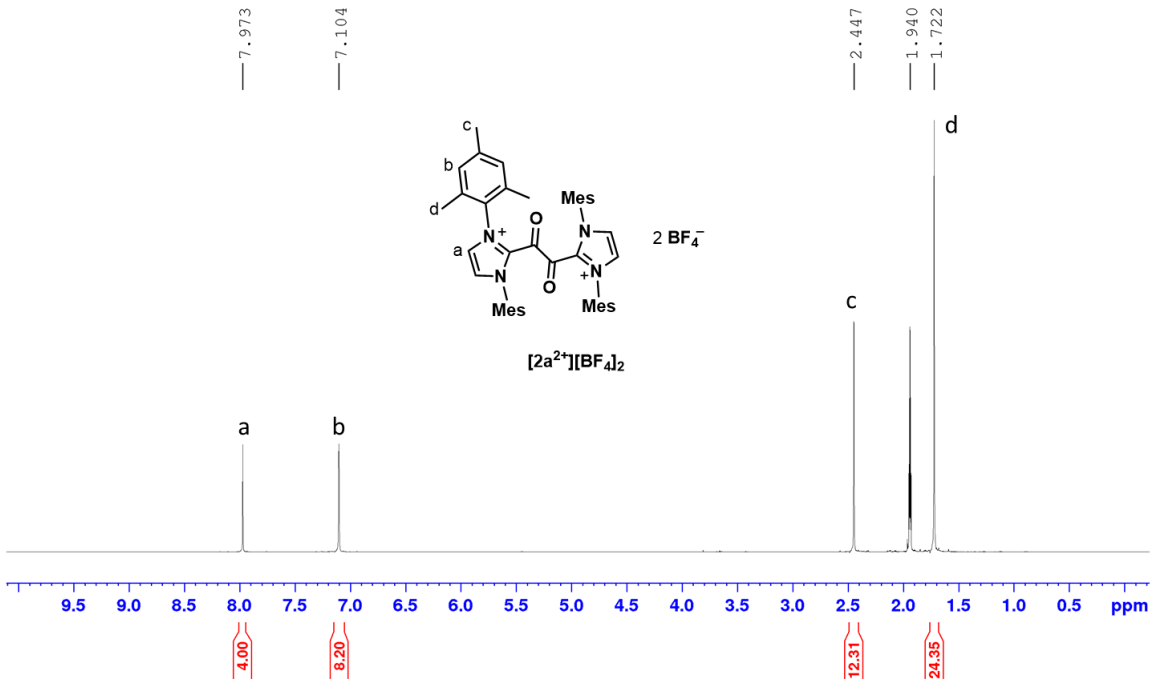

Figure S24. ^{1}H NMR spectrum and assignment of the signals for the compound $[2a^{2+}][BF_4^-]_2$.

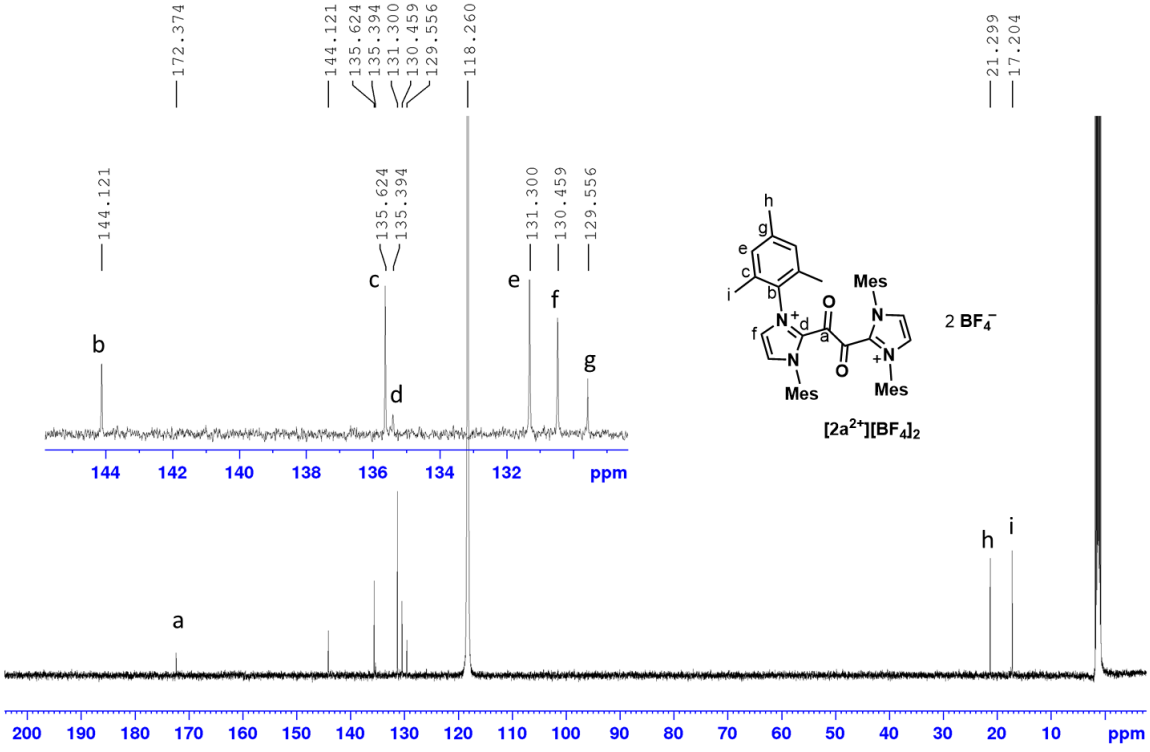

Figure S25. Proton decoupled ^{13}C NMR spectrum and assignment of the signals for the compound **[2a^{2+}][BF$_4^-$]$_2$**.

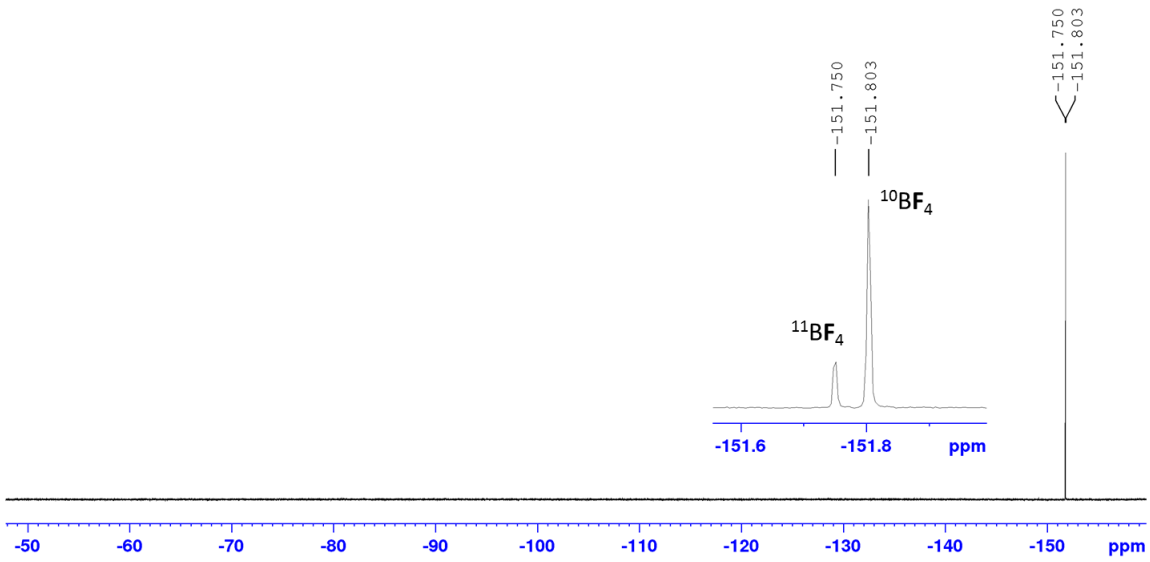

Figure S26. Proton decoupled ^{19}F NMR spectrum for the compound **[2a^{2+}][BF$_4^-$]$_2$**.

^{1}H, ^{13}C NMR spectra of 2a^{0}

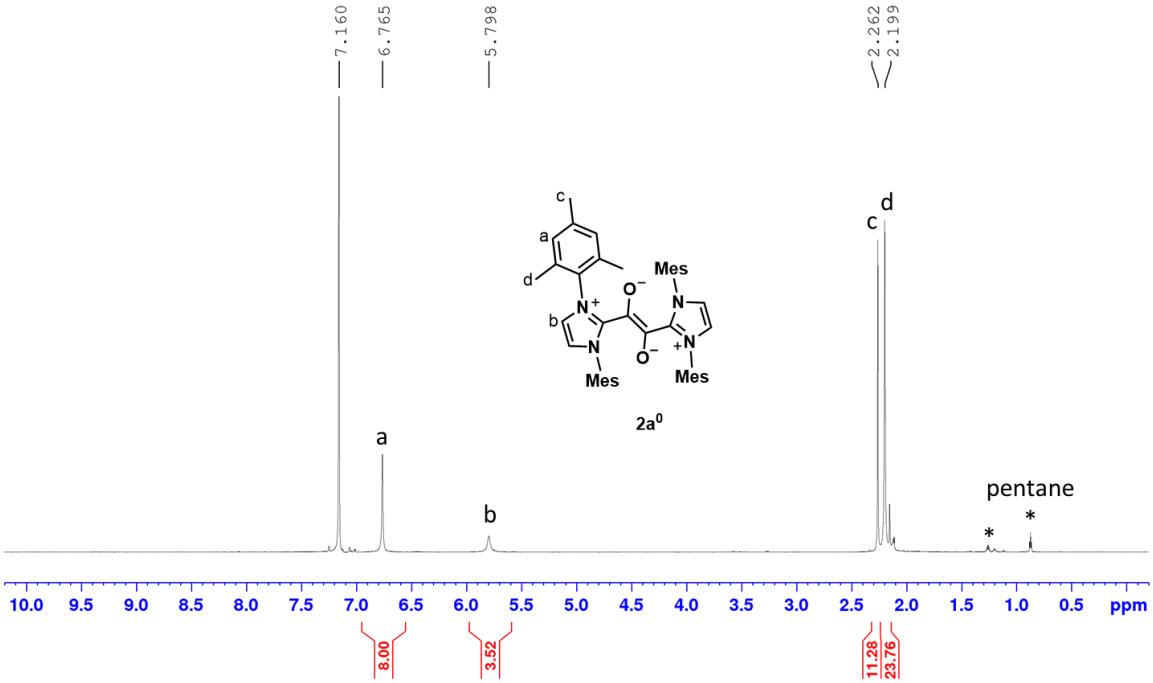

Figure S27. ^{1}H NMR spectrum and assignment of the signals for the compound **2a^{0}**.

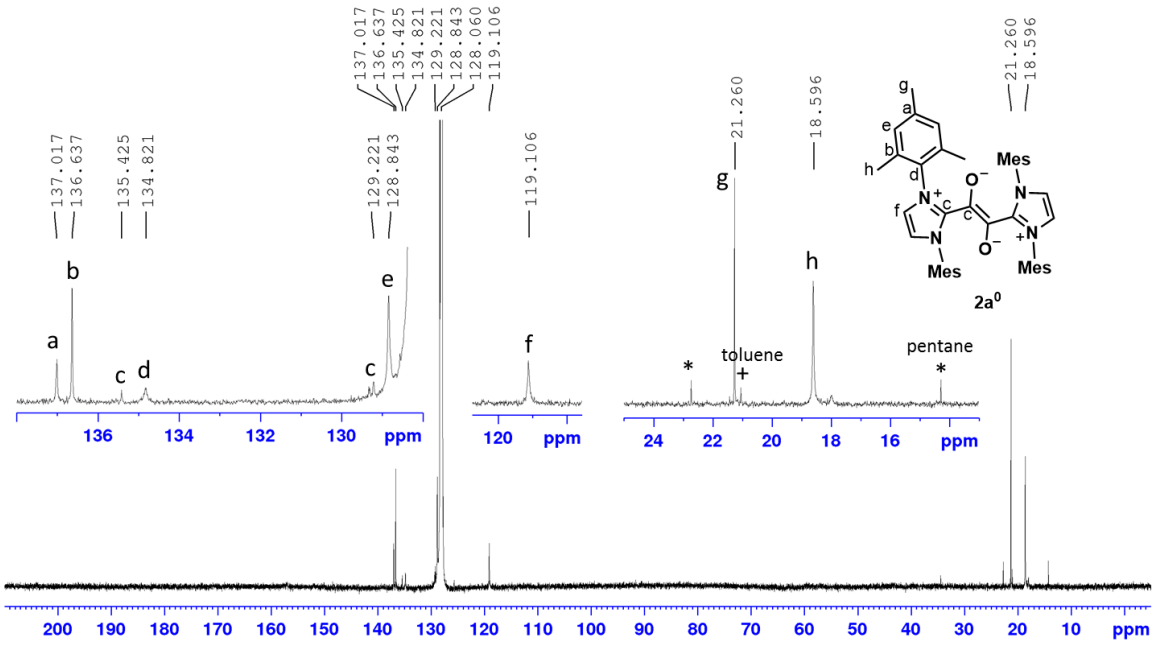

Figure S28. Proton decoupled ^{13}C NMR spectrum and assignment of the signals for the compound **2a^{0}**.

^{1}H, ^{19}F NMR spectra of 2a$^{\bullet+}$

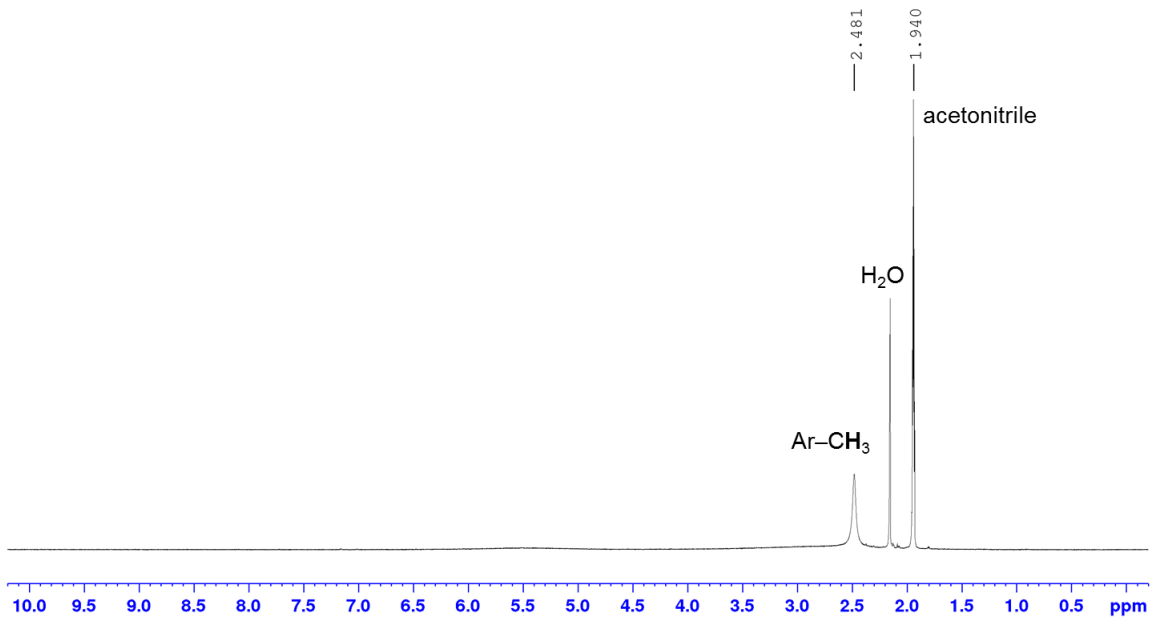

Figure S29. Proton NMR spectrum for the compound **[2a$^{\bullet+}$][Cl^{-}]**.

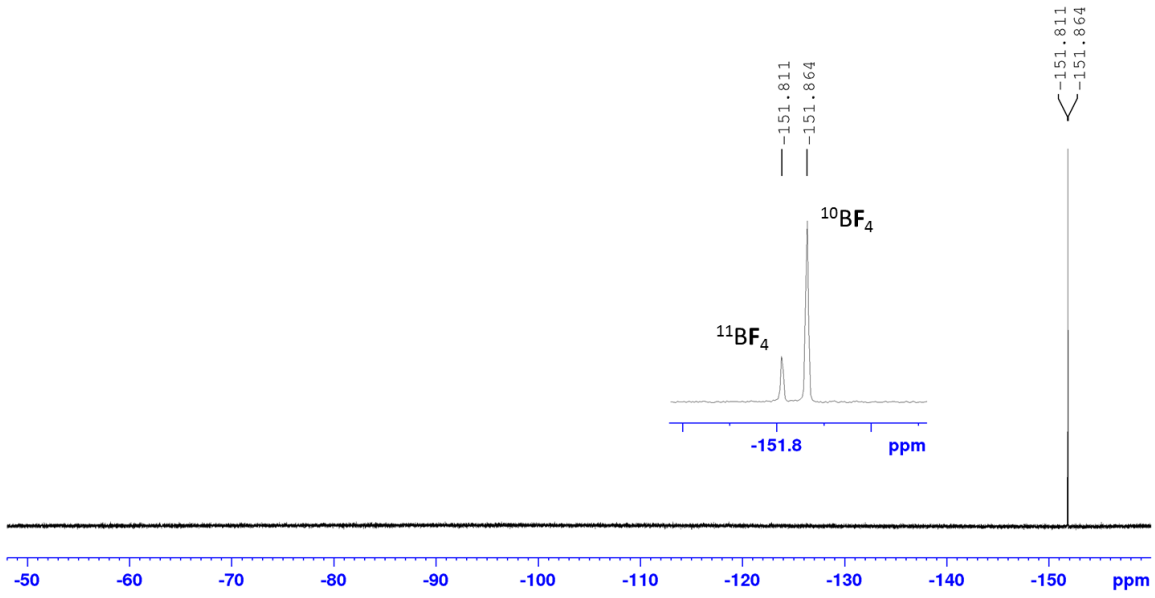

Figure S30. Proton decoupled ^{19}F NMR spectrum for the compound **[2a$^{\bullet+}$][BF$_4^{-}$]**.

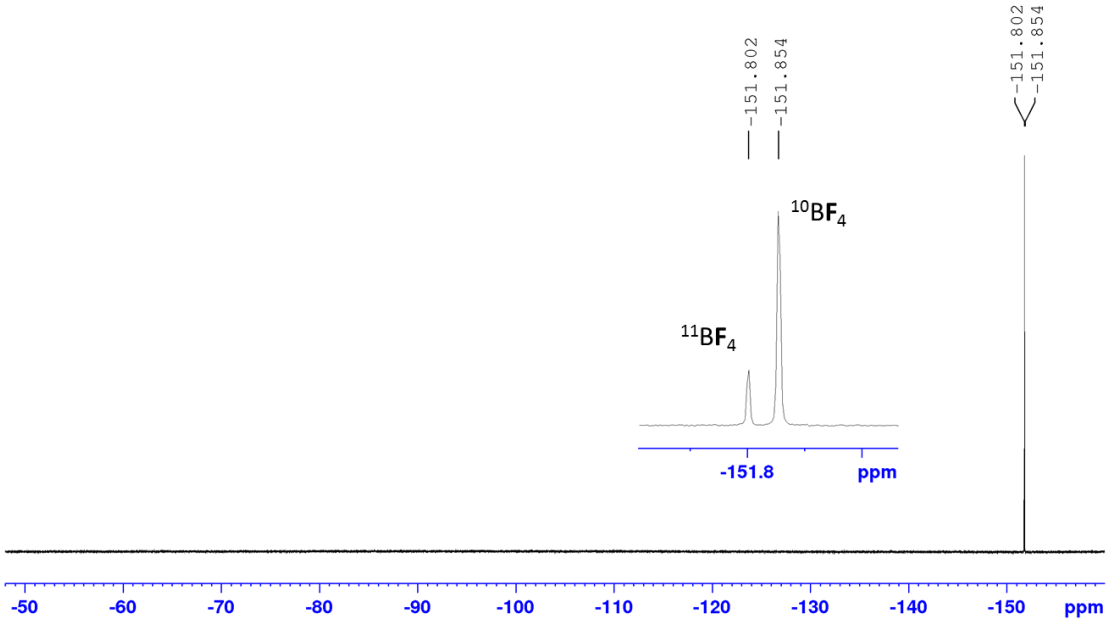

Figure S31. Proton decoupled ^{19}F NMR spectrum for the compound **[2b$^{\bullet+}$][BF$_4^-$]**.

References

[1] X. Bantreil, S. P. Nolan, *Nat. Protoc.* **2011**, *6*, 69-77.

[2] Z. Dong, C. Pezzato, A. Sienkiewicz, R. Scopelliti, F. Fadaei-Tirani, K. Severin, *Chem. Sci.* **2020**, *11*, 7615-7618.

[3] M. J. Frisch, G. W. Trucks, H. B. Schlegel, G. E. Scuseria, M. A. Robb, J. R. Cheeseman, G. Scalmani, V. Barone, G. A. Petersson, H. Nakatsuji, X. Li, M. Caricato, A. V. Marenich, J. Bloino, B. G. Janesko, R. Gomperts, B. Mennucci, H. P. Hratchian, J. V. Ortiz, A. F. Izmaylov, J. L. Sonnenberg, D. Williams-Young, F. Ding, F. Lipparini, F. Egidi, J. Goings, B. Peng, A. Petrone, T. Henderson, D. Ranasinghe, V. G. Zakrzewski, J. Gao, N. Rega, G. Zheng, W. Liang, M. Hada, M. Ehara, K. Toyota, R. Fukuda, J. Hasegawa, M. Ishida, T. Nakajima, Y. Honda, O. Kitao, H. Nakai, T. Vreven, K. Throssell, J. A. M. Jr., J. E. Peralta, F. Ogliaro, M. J. Bearpark, J. J. Heyd, E. N. Brothers, K. N. Kudin, V. N. Staroverov, T. A. Keith, R. Kobayashi, J. Normand, K. Raghavachari, A. P. Rendell, J. C. Burant, S. S. Iyengar, J. Tomasi, M. Cossi, J. M. Millam, M. Klene, C. Adamo, R. Cammi, J. W. Ochterski, R. L. Martin, K. Morokuma, O. Farkas, J. B. Foresman, D. J. Fox, Gaussian, Inc., Wallingford CT, **2016**.

[4] Y. Zhao, D. G. Truhlar, *Theor. Chem. Acc.* **2007**, *120*, 215-241.

[5] F. Weigend, R. Ahlrichs, *Phys. Chem. Chem. Phys.* **2005**, *7*, 3297-3305.

[6] a) G. A. Petersson, A. Bennett, T. G. Tensfeldt, M. A. Al-Laham, W. A. Shirley, J. Mantzaris, *The Journal of Chemical Physics* **1988**, *89*, 2193-2218; b) G. A. Petersson, M. A. Al-Laham, *The Journal of Chemical Physics* **1991**, *94*, 6081-6090.

[7] A. V. Marenich, C. J. Cramer, D. G. Truhlar, *J. Phys. Chem. B* **2009**, *113*, 6378-6396.

[8] T. Lu, F. Chen, *J. Comput. Chem.* **2012**, *33*, 580-592.

[9] a) G. Knizia, *J. Chem. Theory Comput.* **2013**, *9*, 4834-4843; b) G. Knizia, J. E. Klein, *Angew. Chem. Int. Ed.* **2015**, *54*, 5518-5522.

[10] O. V. Dolomanov, L. J. Bourhis, R. J. Gildea, J. A. K. Howard, H. Puschmann, *J. Appl. Crystallogr.* **2009**, *42*, 339-341.

[11] G. M. Sheldrick, *Acta. Cryst.* **2015**, *A71*, 3-8.

[12] G. M. Sheldrick, *Acta. Cryst.* **2015**, *C71*, 3-8.

[13] B. Rees, L. Jenner, M. Yusupov, *Acta. Cryst.* **2005**, *D61*, 1299-1301.

[14] S. Stoll, A. Schweiger, *J. Magn. Reson.* **2006**, *178*, 42-55.

[15] G. R. Fulmer, A. J. M. Miller, N. H. Sherden, H. E. Gottlieb, A. Nudelman, B. M. Stoltz, J. E. Bercaw, K. I. Goldberg, *Organometallics* **2010**, *29*, 2176-2179.